Explosive Impact Analysis

Prefabricated Bunkers as Safe and Efficient Shelter Options

Stan Berghuis

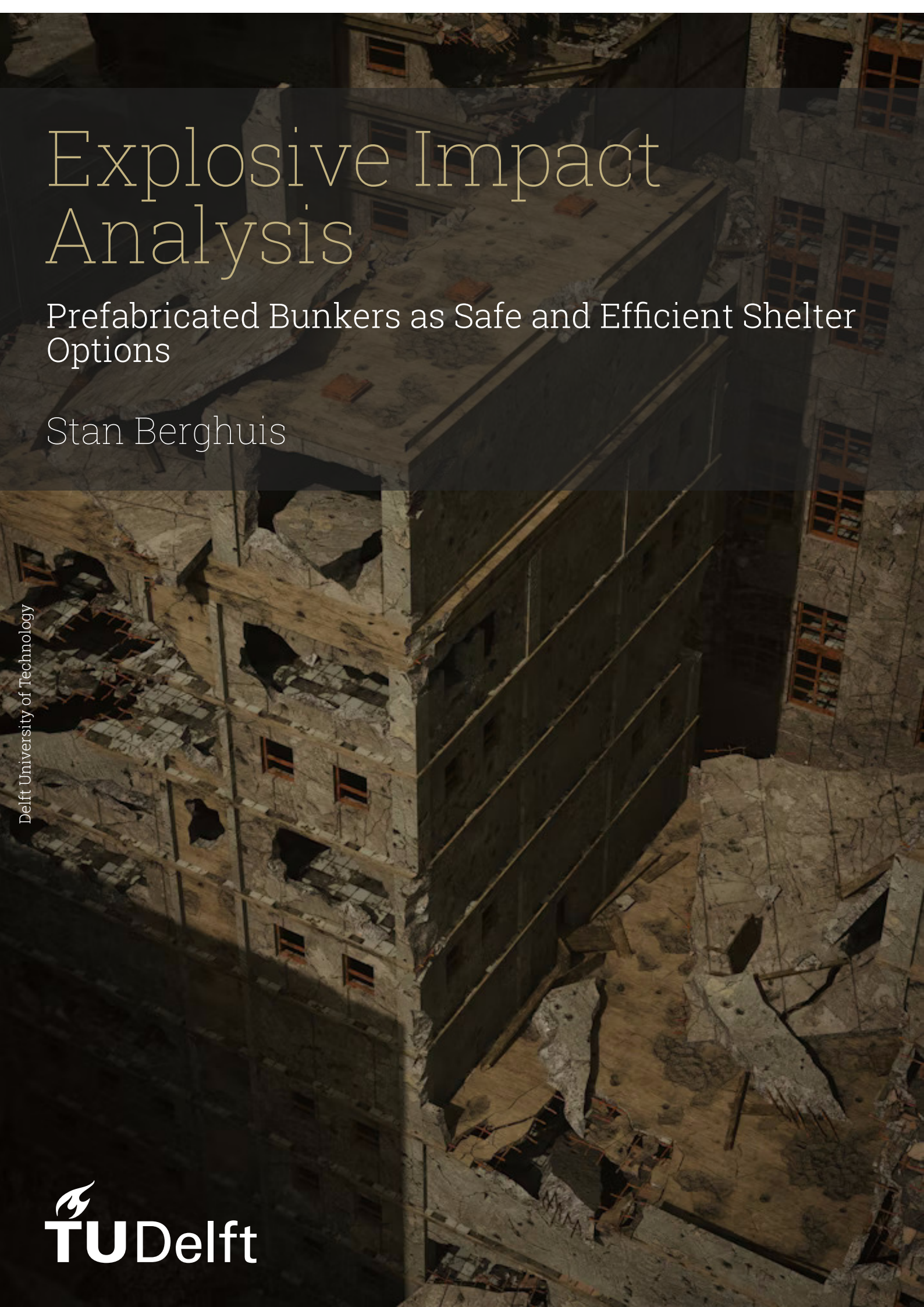

Delft University of Technology

TU Delft

Explosive Impact Analysis

Prefabricated Bunkers as Safe and Efficient Shelter Options

by

Stan Berghuis

Student Number

5602742

Instructor:	Dr.P.C.J. Hoogenboom & dr.ir. M.C.M. Bakker
Project Duration:	July, 2025 - August, 2025
Faculty:	Civil Engineering and Geosciences, Delft

TU Delft

Preface

For language correction and enhancement of academic writing style, AI tools such as ChatGPT were utilized. All substantive ideas, analyses, and conclusions in this thesis are entirely my own.

Stan Berghuis
Delft, August 2025

Summary

This thesis evaluates whether prefabricated shelters, designed for rapid transport and assembly, can provide effective protection against modern explosive threats. This is done by modeling a concrete wall. The study opens with a review of blast physics, covering key parameters needed to model explosions.

Air strikes are increasingly common in modern conflict, especially drone attacks, as shown by recent research. Therefore, the wall design is first subjected to explosive loads from drones.

The structural behavior of a wall with the dimensions of a 20-ft shipping container is analyzed in SCIA Engineer. Through an elastic analysis, the stiffness of the wall is obtained. A hand calculation determines the value at which the wall becomes a mechanism. This value is then put into SCIA to find the corresponding deflection at which plastification occurs. From a different hand calculation, it follows that the wall fails after a displacement of 323.75 mm due to breaking of the reinforcement steel.

A dynamic calculation is made in the form of a mass-spring model. The plastification deflection is taken as the point beyond which the mass–spring system does not return to its original state. The 323.75 mm is the deflection at which the model assumes the wall has failed.

Initial simulations show that the first shelter design fails for all drone explosions occurring closer than approximately 10 meters.

To improve performance, the reinforcement is relocated from the middle of the wall to the tension zone. Besides that a soil layer is added, serving both as camouflage and as additional mass in the dynamic model. With these modifications, the shelter can withstand drone blasts at 5 meters away from the wall (about 2.25 meters away from the outer soil layer). Tests with larger explosives, such as ballistic missiles, indicate that at close standoff distances the shelter does not prevent failure. However, it provides protection at greater distances, starting at 10 meters. This represents a substantial improvement over the initial model, which failed under a relatively small drone impact at the same 10-meter standoff.

Prefabricated shelters can provide effective protection when properly reinforced. Relocating reinforcement to the tension zone and adding a soil layer enhances the blast resilience of the prefabricated shelter. The improved design withstands drone detonations at closer ranges and offers protection against larger explosives at greater standoff distances, demonstrating the potential of prefabricated shelters for civilian protection in modern warfare.

Contents

Preface i

Summary ii

1 Introduction 1
- 1.1 Problem Analysis . . . 1
- 1.2 Objective . . . 1
- 1.3 Methodology . . . 1

2 Explosive Blasts 3
- 2.1 Fundamentals of Explosive Blasts . . . 3
  - 2.1.1 Blast Wave Parameters . . . 3
  - 2.1.2 Spherical vs. Hemispherical Blasts . . . 4
  - 2.1.3 Impact on Environment . . . 4
- 2.2 Explosion Modeling Approaches . . . 5
  - 2.2.1 Modeling methods . . . 5
  - 2.2.2 Scaled Distance and TNT Equivalence . . . 5
  - 2.2.3 Kingery-Bulmash Dataset . . . 6

3 Contemporary Warfare 7
- 3.1 Modern Explosives . . . 7
- 3.2 Missile and Drone Classes . . . 7
  - 3.2.1 Ballistic Missiles . . . 7
  - 3.2.2 Cruise Missiles . . . 8
  - 3.2.3 Hypersonic Missiles . . . 8
  - 3.2.4 Artillery Rockets . . . 8
  - 3.2.5 Loitering Munitions / Drones . . . 8
  - 3.2.6 Artillery Grenades . . . 8
  - 3.2.7 Explosives Summary . . . 8

4 Finite Element Model 9
- 4.1 Boundry Conditions Model . . . 9
- 4.2 Modeling the Wall . . . 9
- 4.3 Elastic Analysis Wall . . . 10
- 4.4 Plastic Analysis . . . 11
  - 4.4.1 Plastic Analysis by SCIA . . . 12
  - 4.4.2 Plastic Analysis Hand Calculation . . . 15
- 4.5 Plastic Analysis for Breaking Point . . . 16

5 Dynamic Analysis 18
- 5.1 Applied Force Calculation . . . 18
- 5.2 Dynamic Analysis . . . 19
- 5.3 Checking the Dynamic Model . . . 21
  - 5.3.1 Checking the Period . . . 21
  - 5.3.2 Influence of Positive Phase Duration and Peak Overpressure . . . 23
  - 5.3.3 Influence of Plastic Spring . . . 24

6 Shelter Improvement 26
- 6.1 Drone Impact on Different Distances . . . 26
- 6.2 Reinforcement Placement . . . 27
- 6.3 Ground Layer . . . 27
- 6.4 Improvement Results on Drone Impact . . . 29

6.4.1 Results with Other Explosives 30
7 Discussion **32**
8 Conclusion **33**
A Python Code Dynamic Response **36**
B Python Code Dynamic Response with Improvements **38**
C Wall Response - Elastic Spring-Mass-Damper **40**
D Python Code With vs Without Plasticity **43**
E Displacement-time Curves for Various Explosives **46**

1 Introduction

1.1. Problem Analysis

In the current geopolitical climate, the assumption of enduring peace in Europe and beyond can no longer be taken for granted. As said by NATO Secretary General Mark Rutte: “We are not at war, but we are certainly not at peace either” (Rutte, 2024). Recent conflicts, such as the ongoing war in Ukraine and the persistent instability in the Middle East, demonstrate a significant shift in the character of warfare, with a pronounced emphasis on aerial threats. Modern conflicts are increasingly characterized by the widespread use of missiles, drones, and precision-guided munitions striking both urban centers and critical infrastructure (Panait, 2024).

Countries such as the Netherlands, which currently have no operational civilian shelters, are especially vulnerable in the face of modern aerial threats. This lack of protective infrastructure leaves both the population and critical services exposed to the destructive impact of contemporary missile and drone attacks. In contrast, neighboring Germany has recently begun preparations to improve its shelter infrastructure. Furthermore, a report presented to the European Commission on October 30th emphasized that member states should enhance their preparedness for such risks, highlighting the urgent need for improved civil protection measures across Europe (NOS Nieuws, 2024).

The construction of permanent shelters is both time-consuming and costly, and their necessity is not a top priority in times of peace. This creates a clear dilemma: investing in such infrastructure may seem unnecessary during stable periods, yet the rapid escalation of conflict can suddenly render these investments critical for national resilience and civilian protection. Hence, it is important for countries to have the infrastructure or an emergency plan as solutions to this rising tension.

1.2. Objective

This report aims to answer the following research question: Can prefabricated shelters, designed for easy transport and assembly, provide protection against modern explosives?

1.3. Methodology

First, the fundamental physics of explosion modeling are reviewed, with reference to current standards and best practices for simulating blast effects. The study then identifies the most commonly used explosives in modern warfare and analyzes their detonation energies to determine the relevant blast loads.

A shelter is modeled with the dimensions of a standard 20-foot shipping container to ensure easy transportability. This also facilitates a straightforward comparison with the use of steel shipping containers instead of concrete shelters for other potential researchers. The structural analysis focuses solely on the walls of shelter.

Structural behavior is modeled in SCIA Engineer, from which the stiffness of the wall is obtained. Using

hand calculations, the load at which the structure enters the plastic regime is determined. Based on the calculated stiffness, the corresponding deflection is found. Failure of the wall is assumed to occur due to the breaking of reinforcement steel, and this critical deflection is calculated manually.

Subsequently, the dynamic response of the wall to blast loading is simulated in Python to assess potential failure. The design is then improved and compared to the previously found results.

Finally, the last design is further analyzed against other explosives to evaluate its behavior under different blast conditions.

2

Explosive Blasts

2.1. Fundamentals of Explosive Blasts

2.1.1. Blast Wave Parameters

Filice et al. (2022) highlight that the understanding of explosion effects has progressed substantially since World War II, largely due to the development and widespread use of various explosives, with Trinitrotoluene (TNT) being the most prevalent. An explosion results in the formation of a blast wave, which is defined by a sudden release of energy that generates extremely high temperatures and pressures. This energy propagates outward in all directions, creating a shock front that moves at supersonic speeds and compresses the surrounding air. The resulting pressure-time profile is characterized by a rapid spike to a peak overpressure, known as the side-on overpressure, followed by an exponential decrease during what is referred to as the positive phase. The length of this positive phase is particularly important when assessing how structures respond to blast loading. The integral of the positive part of the profile is the positive impulse. After this, a longer negative phase occurs, during which the pressure drops below atmospheric levels and can create suction forces. These forces may play a role in damage mechanisms, such as the fragmentation of glass (Filice et al. 2022).

The positive phase is generated as the expanding hot gases from the explosion compress the air, producing a thin, high-intensity shock front. When this shock front encounters a solid object, it can be either reflected or transmitted, with the amount of energy lost depending on the strength and properties of the obstacle.

The time history of the blast overpressure, as seen in Figure 6.2, can be described by the Friedlander equation (Kinney & Graham, 1985):

$$\Delta P(t) = P_{so}\left(1 - \frac{t}{t_p}\right) e^{-b\frac{t}{t_p}} \tag{2.1}$$

where:

- $\Delta P(t)$ = overpressure at time t,
- P_{so} = peak side-on overpressure
- t_p = positive phase duration,
- b = waveform parameter (typically $b \approx 1$),
- t = time after arrival of the shock front.

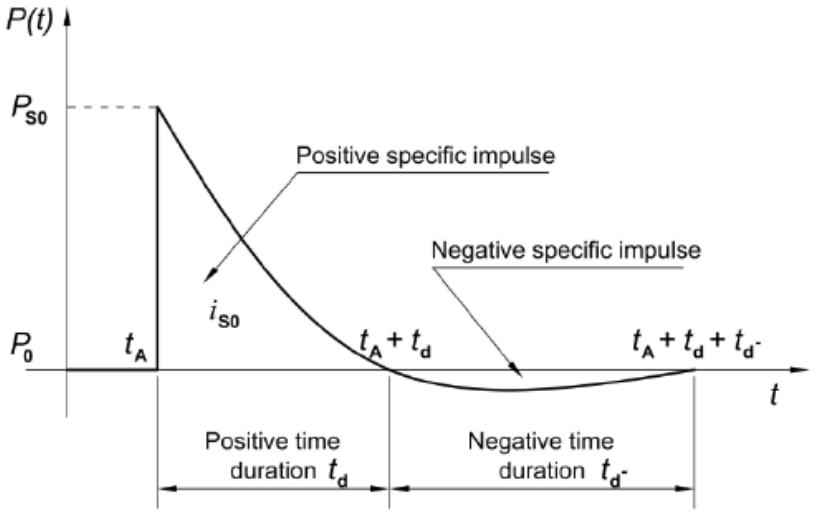

Figure 2.1: Blast wave pressure profile (Trajkovski et al., 2014)

2.1.2. Spherical vs. Hemispherical Blasts

A spherical blast occurs when an explosive detonates in free air, allowing the shock wave to expand equally in all directions. In contrast, a hemispherical blast happens when the explosive is placed on or near a surface, such as the ground, causing the shock wave to reflect and reinforce off the surface. This reflection results in higher peak pressures and impulses near the surface compared to a spherical free-air burst of the same size (Kingery & Bulmash, 1984).

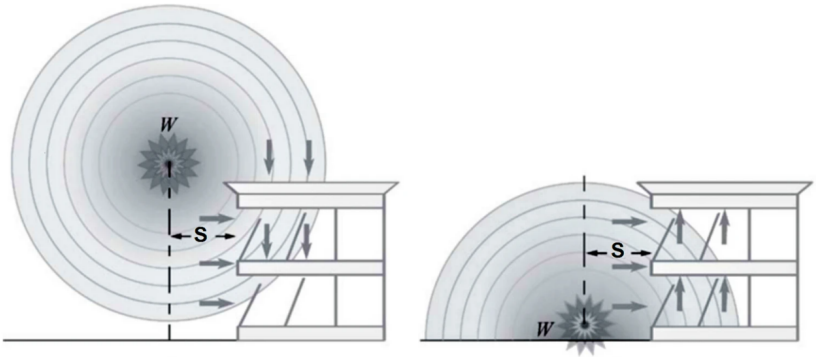

Figure 2.2: Spherical blast (left) and hemispherical blast (right) (Anas & Alam, 2021)

2.1.3. Impact on Environment

Experiments have demonstrated that human tolerance to blast waves is influenced by both the intensity of the blast pressure and the duration of the shock. The lungs are the most critical organ affected by explosive blasts.Blast pressures ranging from 13.8 to 17.2 bar are nearly always fatal on the body. (Catovic & Kljuno Elvedin, 2021)

Damage	Incident Overpressure (psi)
Typical window glass breakage	0.15 – 0.22
Minor damage to some buildings	0.5 – 1.1
Panels of sheet metal buckled	1.1 – 1.8
Failure of concrete block walls	1.8 – 2.9
Collapse of wood framed buildings	Over 5.0
Serious damage to steel framed buildings	4 – 7
Severe damage to reinforced concrete structures	6 – 9
Probable total destruction of most buildings	10 – 12

Table 2.1: Expected damage by blast waves (Kinney & Graham, 1985)

2.2. Explosion Modeling Approaches

2.2.1. Modeling methods

There are several approaches to determine explosion parameters. These include empirical, semi-empirical, and numerical methods. Empirical methods rely mainly on correlations derived from experimental data, but their accuracy tends to decline as the distance from the explosion increases. This method is also limited to the amount and conditions used in the tests. Semi-empirical methods use simplified physical models that capture the key processes involved in explosions. These methods also depend on extensive experimental data and generally provide more accurate predictions than purely empirical approaches. Numerical methods, on the other hand, use mathematical equations that represent fundamental physical laws. They can approximate solutions to non-linear models with a high accuracy, allowing for detailed and precise simulation of explosion phenomena (Filice et al., 2022).

2.2.2. Scaled Distance and TNT Equivalence

The scaled distance and TNT equivalent methods are a widely used semi-empirical approach for modeling explosions. The use of TNT as a reference for determining the scaled distance is a universal method (Draganić & Sigmund, n.d.). The scaled distance and equivalent TNT are calculated as follows:

$$Z = \frac{R}{W_{\text{TNT}}^{1/3}} \tag{2.2}$$

where:

R = distance from the explosion center to the point of interest (ft)
W_{TNT} = TNT equivalent mass of the explosive charge (lb)

$$W_{\text{TNT}} = W_{\text{explosive}} \times \left(\frac{Q_x}{Q_{\text{TNT}}} \right) \tag{2.3}$$

where:

W_{TNT} = equivalent mass of TNT (lb)
$W_{\text{explosive}}$ = actual mass of the explosive (lb)
Q_x = specific energy of the explosive (kJ/lb)
Q_{TNT} = specific energy of TNT (kJ/lb)

Over the years, various formulas have been developed to calculate overpressure and impulse from the scaled distance Z. The existence of multiple methods often leads to different results, highlighting that

there is no single, universally applicable solution. Comparisons of the different methods available are discussed in multiple academic papers to assess the accuracy relative to each other.

2.2.3. Kingery-Bulmash Dataset

The Kingery-Bulmash dataset, published in 1984 as a Ballistic Research Laboratories technical report, is the most comprehensive empirical resource for predicting air blast parameters from TNT explosions. Kingery and Bulmash compiled extensive experimental data from both spherical air bursts and hemispherical surface bursts, covering a wide range of charge sizes and distances. They then fitted this data to high-order polynomial equations, making it possible to calculate key blast parameters—such as peak overpressure, impulse, and positive phase duration—for any scaled distance and charge weight (Kingery & Bulmash, 1984). The polynomial is shown below.

$$Y = 10^{\left(C_0 + C_1 U + C_2 U^2 + \cdots + C_N U^N\right)} \tag{2.4}$$

Here y is the shock wave parameter. This can be the overpressure, impulse, arrival time and phase duration (Jeon et al., 2017).

These polynomial equations and the accompanying tables were quickly adopted by the engineering and safety community. ”The Kingery-Bulmash equation, which is the most widely used equation, has been applied to UFC 3-340-02, a manual published by the U.S. Department of Defense, and Conwep, a blast load estimation software developed by the U.S. Army Corps of Engineers” (Jeon et al., 2017). The tables and graphs found in these documents are either direct reproductions of the Kingery-Bulmash results or are generated using their polynomial fits.The protective design of civilian engineering structures requires the prediction of air-blast loadings. Therefore in this research the design tables of Kingery and Bulmash will be taken for the calculation of the key parameters. Figure 2.3 shows how these tables look for a spherical and hemispherical blast.

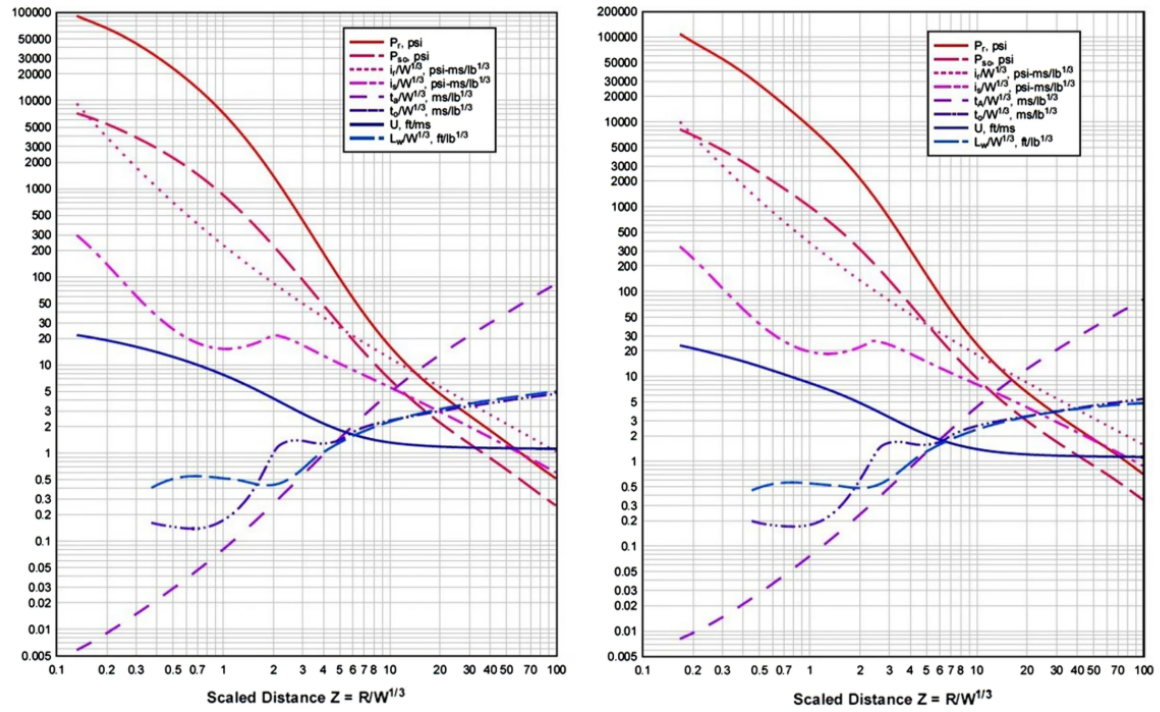

Figure 2.3: Design graphs for blast parameters, hemispherical (left) and spherical (right) (US, 2008)

The dark pink dotted line (second from top), Pso, is the free-air overpressure; the dotted purple line (second from bottom) indicates $t0$, the positive phase duration. These parameters enter equation 2.1 to model the explosion pressure–time history. For the dynamic model in Chapter 5, Pr (upper solid red line) is used, the reflected pressure on the wall, which exceeds free-air pressure due to wave reflection.

3

Contemporary Warfare

3.1. Modern Explosives

Modern warfare has evolved in the 21st century into a domain characterized by rapid technological advancements that have fundamentally changed the nature of conflict. The integration of unmanned systems, particularly drones (unmanned aerial vehicles or UAVs), and precision-guided munitions has shifted military strategies (NatStrat, 2021).

Recent conflicts, from Ukraine to several theaters in the Middle East, illustrate this trend. In Ukraine, for example, the widespread use of drones has demonstrated their effectiveness for real-time surveillance and targeted strikes, with production plans aiming at building millions of inexpensive FPV drones by 2025 (Axe, 2025). In the Middle East, Iranian-manufactured Shahed drones and similar systems have introduced a new era of accessible, low-cost, and high-impact weaponry, allowing even minor groups to undertake sustained aerial campaigns (Crowley & Crowley, 2025).

Guided missiles play an equally pivotal role. Precision-guided munitions are increasingly deployed to neutralize specific targets with minimal collateral damage. Instances such as Russia's use of Kalibr and Iskander missiles in Ukraine, and Western systems like HIMARS demonstrating accurate, long-range strikes, underscore the strategic revolution in missile technology.

3.2. Missile and Drone Classes

Below is an overview of the different missile and drone classes. Each class includes various types with differing ranges and warhead masses. For design purposes, the strongest system identified within each class is used as the reference point.

3.2.1. Ballistic Missiles

· **Short-Range Ballistic Missiles (SRBM):** SRBMs are ballistic missiles with a range of 300–1,000 km, used for tactical or regional strikes (Wikipedia contributors, 2025). An example is the Iskander-M (Russia), which carries a warhead of 700 kg (Gluck, 2024).

· **Medium-Range Ballistic Missiles (MRBM):** MRBMs have ranges between 1,000 and 3,500 km and are used for regional deterrence and strategic strikes (Wikipedia contributors, 2025a). The strongest example is the Shahab-3 (Iran), with a warhead mass of 1,200 kg (Shaikh, 2024).

· **Tactical Ballistic Missiles:** Tactical ballistic missiles are short-range missiles (typically under 300 km) for battlefield use, targeting enemy forces and infrastructure (Wikipedia contributors, 2025a). The strongest example is the Tochka-U (SS-21 Scarab, Russia), with a warhead mass of 482 kg (Shaikh, 2024a).

3.2.2. Cruise Missiles
Cruise missiles are guided missiles that fly at low altitude and constant speed, designed for precision strikes (Wikipedia contributors, 2025c). The strongest example is the Tomahawk Block IV (USA), with a warhead mass of 450 kg (Dahlgren, 2024).

3.2.3. Hypersonic Missiles
Hypersonic missiles travel at speeds greater than Mach 5 and are designed to evade modern air defenses (Wikipedia contributors, 2025c). The strongest example is the Kinzhal (Russia), with a warhead mass of 480 kg (Dahlgren, 2024a).

3.2.4. Artillery Rockets
Artillery rockets are unguided or guided rockets used for battlefield support, typically with ranges under 100 km. The strongest example is the BM-30 Smerch (Russia), with a warhead mass of 100 kg (Wikipedia contributors, 2025a).

3.2.5. Loitering Munitions / Drones
Loitering munitions, or ”kamikaze drones,” are unmanned aerial vehicles designed to loiter over the battlefield and strike targets by self-destruction. The Shahed-136 (Iran) is a widely used example, featuring a range of up to 2,500 km and carrying a warhead of approximately 40–50 kg. It has been extensively deployed in Ukraine and the Middle East, where its low cost and mass production have enabled persistent attacks on both military and civilian infrastructure (Wikipedia contributors, 2024).

3.2.6. Artillery Grenades
Artillery grenades, also known as high-explosive (HE) shells, are commonly used in modern artillery systems for indirect fire support. A typical 155 mm HE artillery shell contains approximately 6.6 kg of TNT as its explosive filler (Defense, 2025).

3.2.7. Explosives Summary
In Table 3.1, it is assumed that all warheads contain 100% TNT as their explosive filler. In reality, the exact composition of warheads can vary, with many using alternative or mixed explosives. These can be converted to TNT equivalence using Formula 2.2. However, due to the variability and limited public data on specific compositions, a 100% TNT assumption is applied for consistency in this analysis.

System	Warhead TNT (kg)
Iskander-M	700
Shahab-3	1200
Tochka-U	482
Tomahawk	450
Kinzhal	480
BM-30 Smerch	100
Shahed-136	50
155 mm HE Artillery Grenade	6.8

Table 3.1: Strongest explosives in each class with warhead TNT equivalents, assuming the explosive in the warhead is TNT.

4

Finite Element Model

4.1. Boundry Conditions Model

Before starting the modeling process, it is important to carefully select which loads to consider. Given that missiles are costly and unlikely to be used indiscriminately, the primary concern is the increasing prevalence of drone attacks. Therefore, the initial analysis will focus on the impact of a drone explosion on the bunker wall. After this, the structural response to incoming missiles and artillery will also be examined to assess the bunker's performance under more severe loading scenarios.

Ground detonation and near-surface detonation both result in a hemispherical blast wave and can be analyzed using the same methods. For the purposes of this study, these scenarios are considered equivalent and are modeled as a surface burst near the structure. The structural model will consider near-surface / ground detonation as the primary loading scenario.

4.2. Modeling the Wall

For the analysis, a prefab shelter with the same dimensions as a 20-foot shipping container is used. The shelter measures 6060 mm in length and 2590 mm in height, with walls made of 200 mm thick C45/55 concrete (see Figure 4.1).

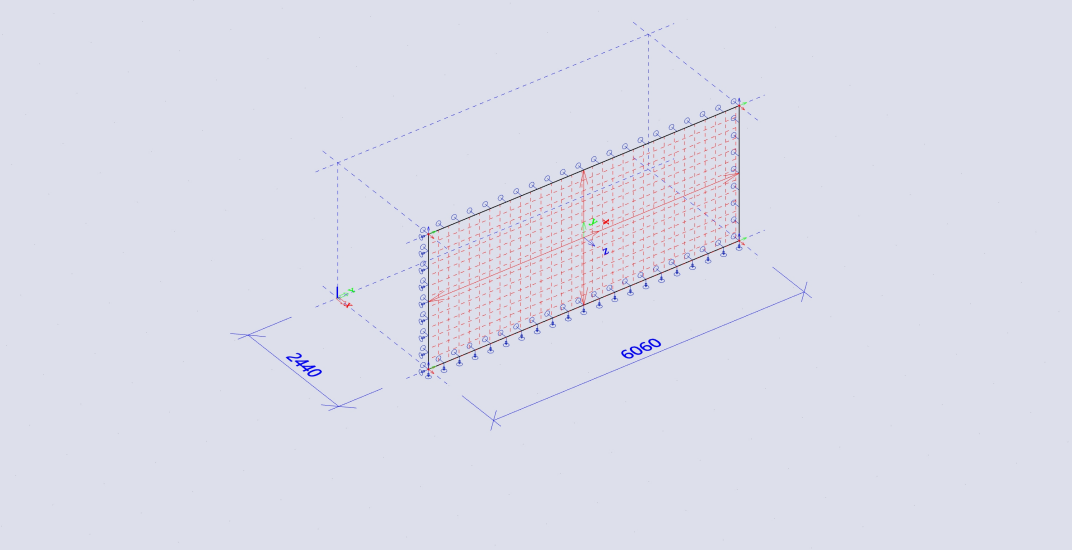

Figure 4.1: Concrete wall with reinforcement steel (SCIA Engineer)

The wall is capable of rotating about each axis. It is fixed in the X direction. At the bottom, the wall is

restrained in the Z direction due to its connection to the foundation, while translation in the Y direction is free to allow for shrinkage, thermal expansion, and other movements. On the left side, a spring support with low stiffness is applied in the y direction to stabilize the structure. This setup models the wall as a freely supported plate.

The reinforcement dimensions are based on a first guess. Based on the initial results, some variables are tweaked in Chapter 6. For the steel, B500B is chosen with a diameter of 12 mm. The placement of the steel is initially assumed to be in the middle of the wall. There is a coverage of 100 mm from the side surface on both sides. The bars are spaced at 200 mm center-to-center, with a construction tolerance of ±10 mm. Given the wall length of 6060 mm, this results in approximately 30 bars placed along the wall.

4.3. Elastic Analysis Wall

The primary objective of the elastic analysis is to determine the wall's stiffness. This stiffness value will subsequently be utilized in the dynamic analysis of the structure. Elastic behavior of a material is characterized by the ability to return to its original state upon unloading. In this phase, the stiffness can be determined as the slope of the force-displacement graph.

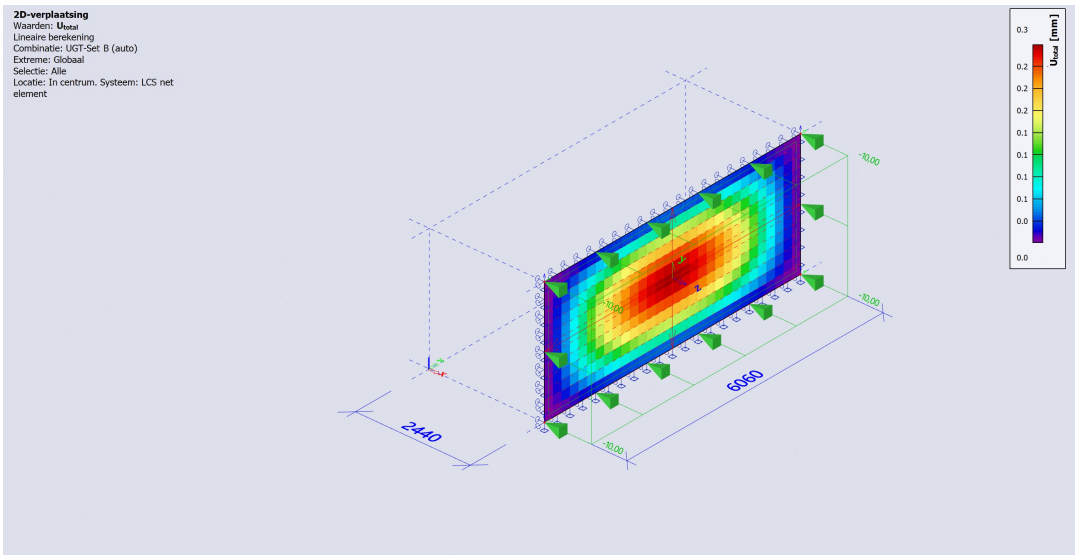

Figure 4.2: Total deformation at 10 kN/m^2 (SCIA Engineer)

The stiffness k is calculated as:

$$k = \frac{F}{U_{\text{total}}} = \frac{P \times A}{U_{\text{total}}} \tag{4.1}$$

Given a pressure of $P = 10\,\text{kN/m}^2$ applied on a wall with area A. Not all force works directly on the wall, some parts go into the supports. It is assumed that 70% of the length and height works on the wall. Therefore, the area is reduced by 0.7 x 0.7.

The area A is:

$$A = 6060 \times 2590 \times 0.7 \times 0.7 = 7,690,746\,\text{mm}^2 = 7.69\,\text{m}^2$$

It is important to note that SCIA assumes uncracked concrete behavior which is not realistic for explosive analysis. Generally the E-modulus of concrete should be reduced by a factor of one third when the reinforcement bars are positioned normally, that is located in the tension zone rather than in the middle as assumed here.

For this special case the E-modulus of a wall with cracked concrete is estimated by modeling the original 200 mm thick wall in SCIA Engineer as a 100 mm thick wall with the reinforcement placed in the middle. This approach simulates the effective cracked concrete section.

Using SCIA, displacement values U are obtained for both the full 200 mm and the reduced 100 mm wall models. Then, applying formula 4.1, two stiffness values k are calculated. The ratio between these stiffness values corresponds to the ratio between the cracked and uncracked E-moduli.

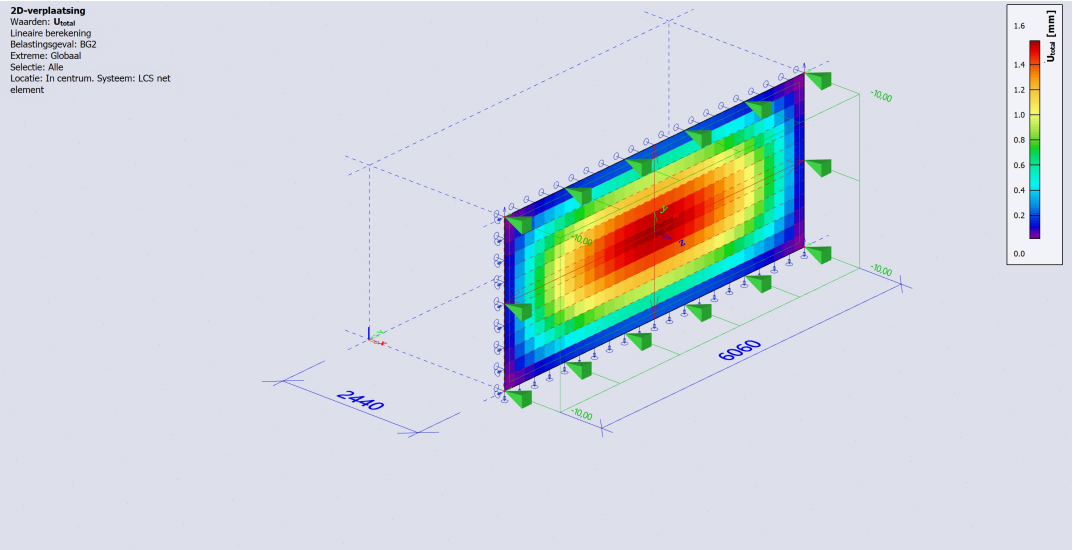

Figure 4.3: Total deformation at 10 kN/m^2 on reduced thickness of 100mm (SCIA Engineer)

The stiffness ratio between the two cases is $1 : 8$. The factor 8 accounts for the geometric reduction. After this geometric reduction, an additional factor 3 is applied to represent the further loss of effective stiffness due to concrete cracking. The total multiplier on deflection is $8 \times 3 = 24$, so

$$U_{\text{cracked}} = 24\, U_{\text{uncr}} = 24 \times 0.0002\ \text{m} = 0.0048\ \text{m}.$$

The total force F is:

$$F = P \times A = 10\,\text{kN/m}^2 \times 7.68804\,\text{m}^2 = 76.88\,\text{kN}$$

Finally, the stiffness k is:

$$k = \frac{76.88\,\text{kN}}{0.0048\,\text{m}} = 16.017\,\text{KN/m}$$

4.4. Plastic Analysis

After the elastic phase, the structure enters the plastic regime. Initially, one reinforcement bar begins to yield. This may already have occurred during the elastic phase, but the overall structure still behaves elastically. Once all the reinforcement bars start yielding, a plastic mechanism forms. The point at which this mechanism develops is critical for plastic analysis. After the mechanism forms, strain continues to increase until a bar eventually fractures. When a bar breaks, the tensile capacity of the wall drops sharply, causing the remaining bars to fail in sequence. This progressive failure ultimately leads to the collapse of the wall.

The calculations done in SCIA Engineer are based on static loading conditions. An explosion is a dynamic scenario so the values found can not be used in the final calculations, they are used to get a feeling of the order of magnitude. In the settings non-linear material properties for concrete and steel are used. Besides that it is assumed that the concrete has zero tensile strength so the entire tensile force is taken by the reinforcement steel.

4.4.1. Plastic Analysis by SCIA

For the plastic analysis in SCIA, the force on the wall is increased incrementally until a small increase in force results in a large increase in deflection indicating a mechanism has formed.

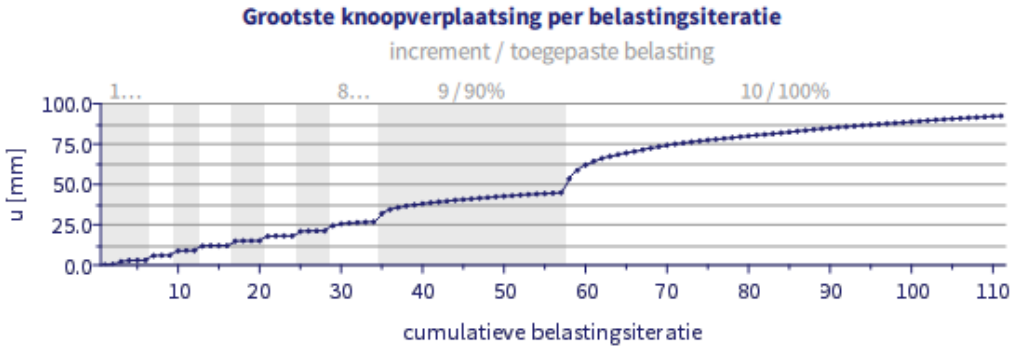

Figure 4.4: 50 KPa loading, deformation against iteration chart (SCIA Engineer)

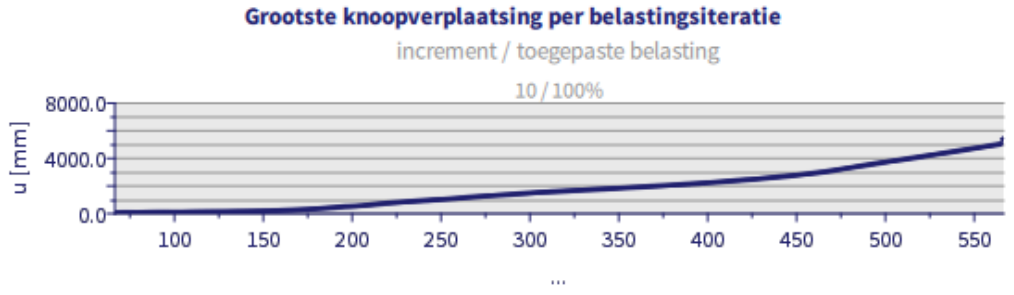

Figure 4.5: 51 KPa loading, deformation against iteration chart (SCIA Engineer)

As seen in the figures above the loading situation with 50 KPa gives a deformation of 94.3 mm. When we increase the load by 1 KPa to 51 KPa the graph keeps iterating showing very large deflections. This means the structure has become a mechanism under static loading. A small increase in force gives a very large deflection. This is typical for the plastic regime as can be seen from figure 4.7.

To assess the condition of the reinforcement steel just before the structure forms a mechanism, a pressure of 50 kPa is applied to the wall. The maximum strain observed in the reinforcement bars is 4.518×10^{-2} (4.518%), occurring in the y-direction (vertical along the wall). This value is well below the critical strain threshold of 0.25 (25%), at which the steel reinforcement bars would break. The strain indicates that some bars are yielding, as expected from the explanation above. Therefore, it can be concluded that at 50 kPa the steel is not broken and some bars have started to yield. When all bars yield, a mechanism forms, which occurs at 51 kPa, as shown in Figure 4.4.

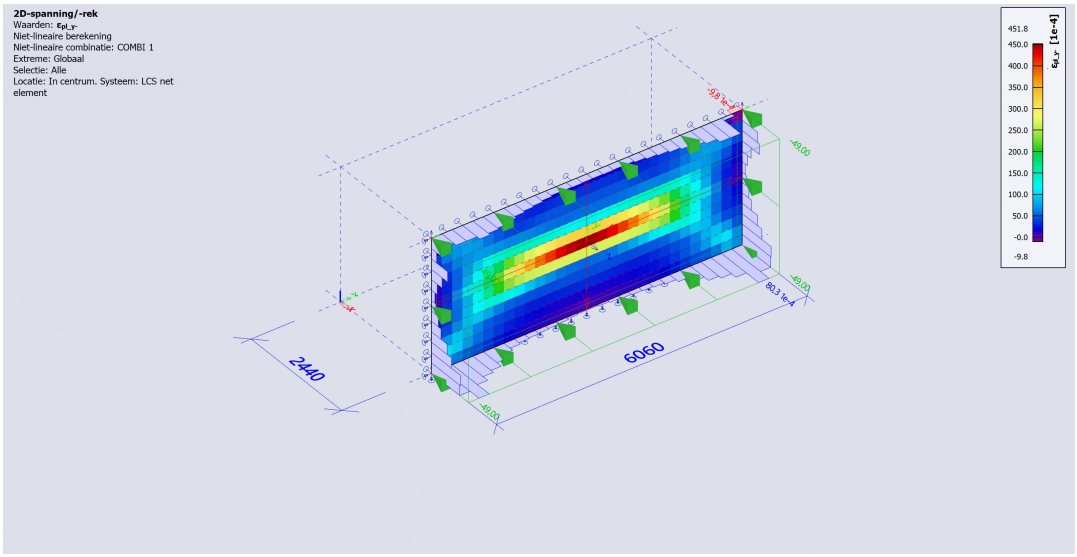

Figure 4.6: Strain in reinforcement bars in the y-direction (local axis) under 50 kPa loading (SCIA Engineer).

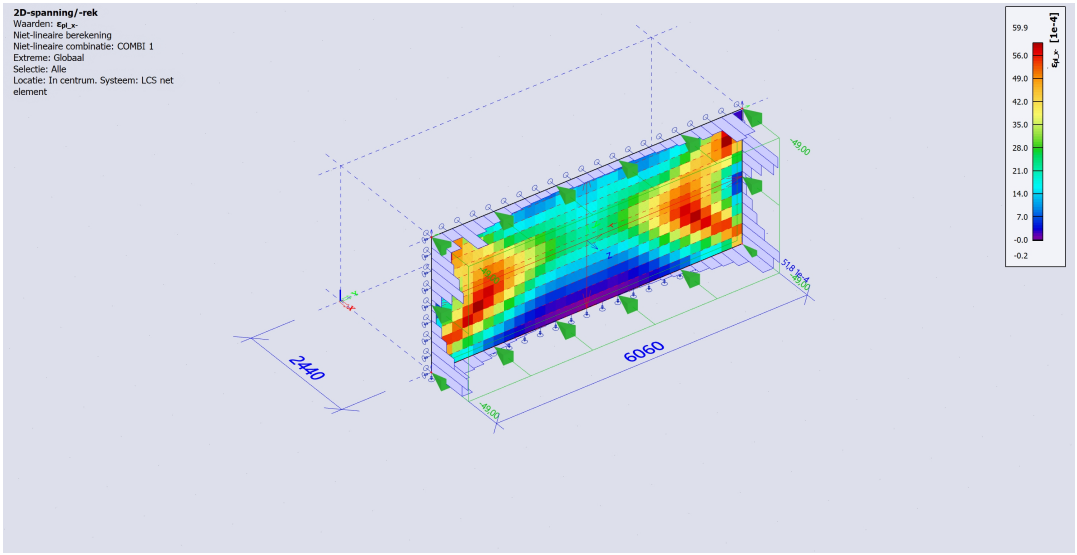

Figure 4.7: Strain in reinforcement bars in the x-direction (local axis) under 50 kPa loading (SCIA Engineer).

A typical force-displacement curve can be seen in the figure below.

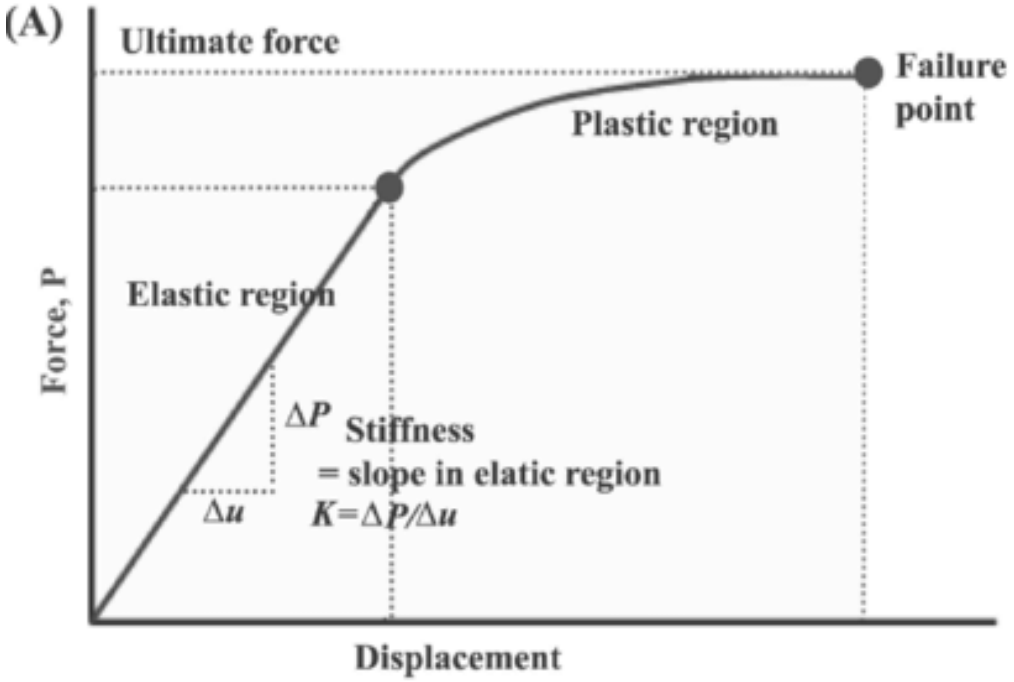

Figure 4.8: Typical force-displacement diagram

In the elastic region the force and displacement are linearly connected to each other by the stiffness found in section 4.3, once plastic deformation, now called Upl, is reached there is no linear behavior anymore. A small increase in force gives a large increase in deflection, this happens until the failure point $Ubreak$.

To simplify this, the force-displacement curve can be approximated as bi-linear, as shown in the image below.

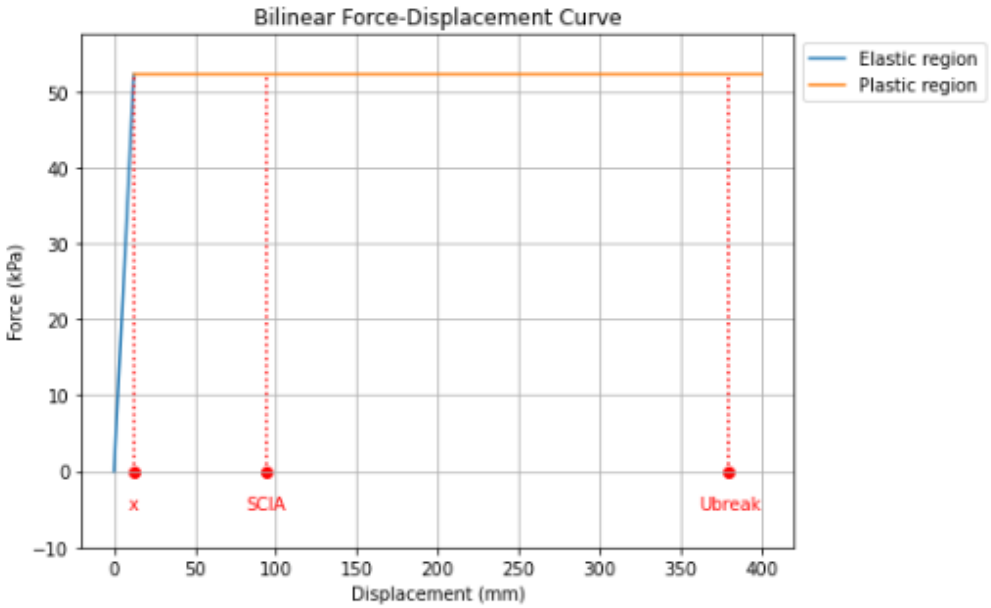

Figure 4.9: Bi-linear force-displacement diagram (Python).

To visualize the values found so far, a Python plot is made. Point x is the point where the behavior of the structure goes from elastic to plastic (Upl). The SCIA point is the point where a mechanism forms under static loading conditions. $Ubreak$ is the point where the steel reinforcement bars break and the structure fails.

4.4.2. Plastic Analysis Hand Calculation

The value of 51 KPa found by SCIA Engineer has to be validated with a hand calculation.

$$A_{s,\text{bar}} = \frac{\pi}{4} d^2 \tag{4.2}$$

$$A_{s,\text{bar}} = \frac{\pi}{4} \times (0.012)^2 = 0.000113 \text{ m}^2$$

The amount of bars per meter is calculated. There is a spacing of 0.2 m between every bar.

$$n = \frac{1}{0.2} = 5$$

$$A_{s,1m} = 5 \times 0.000113 = 0.000565 \text{ m}^2$$

The moment capacity of the wall is determined using the following formula. Since the wall is longer than it is tall, only the vertical reinforcement bars are considered in the calculation. The resulting capacity is expressed in kNm/m.

$$m_p = A_{s,1m} \cdot f_{yd} \cdot z \tag{4.3}$$

$$m_p = 0.000565 \times 435 \times 10^6 \times 0.1 = 24,577.5 \text{ Nm/m} = 24.6 \text{ kNm/m}$$

The formula for the failure load is taken from the lecture notes on plasticity by Vrouwenvelder and Witteveen (2003):

$$w_u = \frac{72}{5} \cdot \frac{m_p}{a^2} \tag{4.4}$$

$$w_u = 14.4 \cdot \frac{24,600}{2.59^2} = 14.4 \cdot 3,666.6 = 52,800 \text{ N/m}^2 = 52.8 \text{ kPa}$$

This formula is valid for a height to width ratio of 1:2. For the case of this wall, the ratio is 1:2.34. So, the formula is an approximation, chosen to be valid since the ratios are relatively close to each other.

The deflection caused by this force can be estimated using formula 4.5, which is a standard expression for simply supported beam deflection. Applying it to a wall is a significant simplification, and the calculation serves primarily to verify the order of magnitude of the deflection found by SCIA.

$$u = \frac{5}{384} \frac{ql^4}{EI} \tag{4.5}$$

where:

- $u =$ displacement
- $q =$ load
- $l =$ length
- $E =$ Young's modulus
- $I =$ moment of inertia

C45/55 concrete has a Young's modulus (E-modulus) of 36,300 MPa. In this calculation, it is assumed that the concrete is cracked, so the effective stiffness is taken as one-eight of the original modulus. Filling in the formula gives:

$$u = \frac{5}{384} \cdot \frac{52.8 \times 10^3 \,\text{N/m} \cdot (2.59\,\text{m})^4}{4537.5 \times 10^6 \,\text{N/m}^2 \cdot \frac{1}{12} \cdot 1.00\,\text{m} \cdot (055.20\,\text{m})^3}$$

$$u \approx 0.01022\,\text{m} = 10.22\,\text{mm}$$

Accounting for the cracking gives:

$$u \approx 0.03067\,\text{m} = 30.68\,\text{mm}$$

From the hand calculation, it follows that $U_{pl} = 30.68$ mm. As mentioned earlier, this is a simplification intended only for comparison with the results from SCIA. The SCIA calculations incorporate all boundary conditions without simplifying the equations. When a pressure of 52.8 kPa is applied to the wall, an elastic analysis (neglecting plastification) shows a deflection of 1.1 mm at the center of the wall. Multiplying this by 24 to account for cracked concrete and reduced stiffness yields $U_{pl} = 26.4$ mm. Since SCIA provides a more accurate result, this value will be used in the dynamic calculation.

The difference between the hand calculation and SCIA results is approximately 13.95%, which confirms that the simplified model is valid to use. The moment where SCIA becomes a mechanism shows how the bi-linear diagram works. Figure 4.9 shows a small increase in force after the x point gives a big difference in deflection. This happens at Upl.

4.5. Plastic Analysis for Breaking Point

To find the deflection at which the bars break ,$Ubreak$, a hand calculation must be performed. In SCIA Engineer, the breaking of reinforcement bars cannot be modeled. The model becomes unstable before the bars actually break, making it impossible to determine the exact point of failure.

From the geometry of the folded construction, the relationship between the deflection u, the length l, the width of the fold w, and the height h is given by:

$$\frac{u}{l/2} = \frac{w/2}{h/2} \tag{4.6}$$

A drawing illustrating the derivation of this formula can be found in Figure 4.9. This drawing was created by Dr. P.C.J. Hoogenboom for a beam. The formulas have been adapted to suit the scenario of the wall.

Formula 4.6 leads to:

$$u = \frac{l}{2} \cdot \frac{w}{h} \tag{4.7}$$

The fracture strain of steel is assumed to be 25%, that is:

$$\epsilon_{\text{fracture}} = \frac{w}{h} = 0.25 \tag{4.8}$$

Substituting this into the formula for u gives the deflection at fracture:

$$u_{\text{break}} = \frac{l}{2} \cdot 0.25 = 0.125l \tag{4.9}$$

For a length $l = 2590$ mm:

$$u_{\text{break}} = 0.125 \times 2590 = 323.75 \text{ mm}$$

When $Ubreak$ is reached the structure has failed due to the reinforcement breaking resulting in a loss of tensile strength.

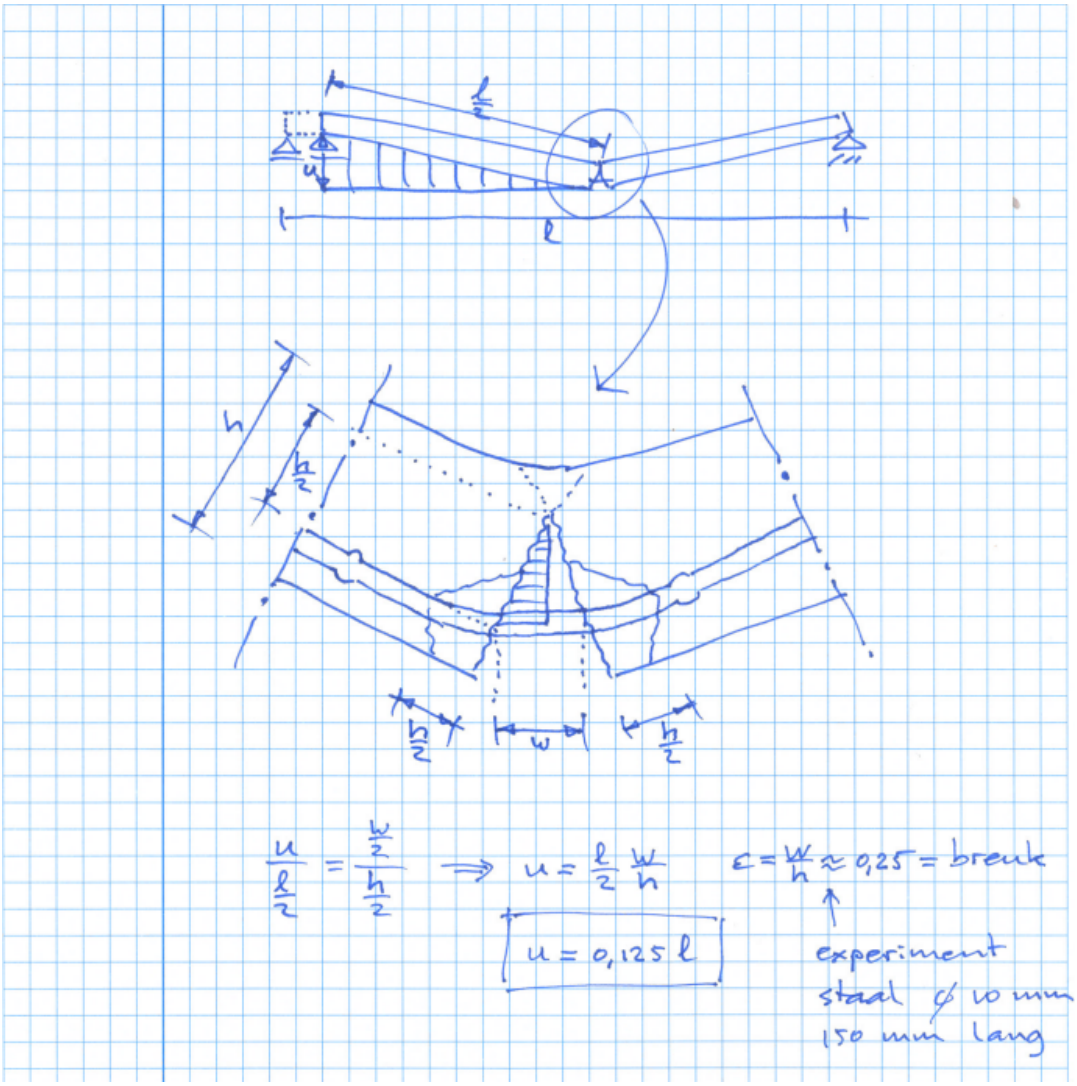

Figure 4.10: Derivation of $Ubreak$ formula by Dr.P.C.J. Hoogenboom

5

Dynamic Analysis

5.1. Applied Force Calculation

The wall is made of concrete C45/55. The scaled distance for a hemispherical blast 1 meter away from the structure is:

$$Z = \frac{R}{W^{1/3}}$$

where:

- $R = 1$ m
- $W = 50$ kg

It is important to convert W from kg to lb and R from m to ft. So,

$$W^{1/3} = (110\,\text{lb})^{1/3} \approx 4.79\,\text{lb}^{1/3}$$

$$R = 1\,\text{m} = 3.28084\,\text{ft}$$

$$Z = \frac{3.28084\,\text{ft}}{4.79\,\text{lb}^{1/3}} \approx 0.685\,\text{ft/lb}^{1/3}$$

Looking at Figure 4.6, the following parameters are obtained for the calculated scaled distance:

- Peak reflected overpressure: $P_r = 19000$ psi $= 131$ MPa
- Positive phase duration: $t_0 = 0.86$ ms

When the shock hits the wall, it reflects and further compresses the air at the surface, creating pressures several times higher than the free-field Pso. The wall is therefore loaded by Pr, using Pso would underestimate the pressure (2008, UFC 3-340-02). Normally Pr is a function of Pso but since it is assumed that the blast wave hits the wall perpendicular the alpha factor is zero and the Pr value found in figure 5.1 can be taken.

These values will be used to model the explosion with formula 2.1.

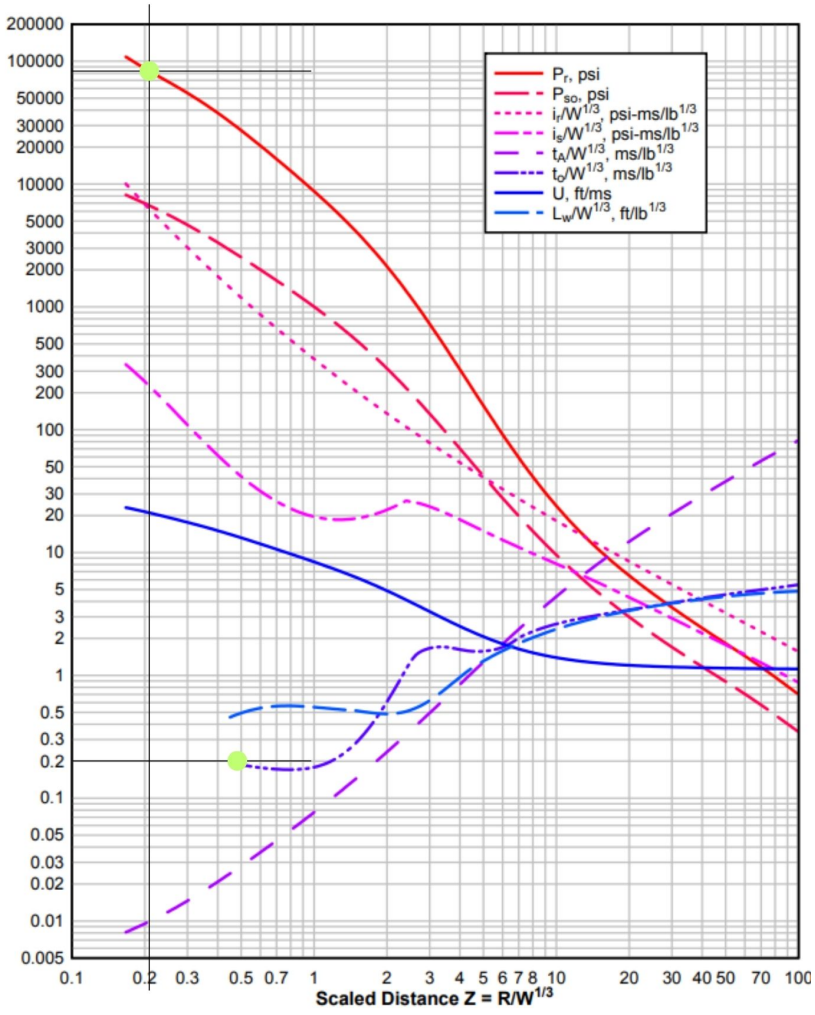

Figure 5.1: Intersection, scaled distance and parameter curves

5.2. Dynamic Analysis

For the dynamic analysis, the previous calculations are incorporated into a mass-spring model, where the dynamic pressure from the explosion (see formula 2.1) is applied to the wall to determine its response. The wall is modeled as a single degree-of-freedom system, consisting of a mass m (representing the relevant portion of the wall), a spring with stiffness k (representing the elastic behavior of the wall), and a damper with damping constant c (representing energy dissipation).

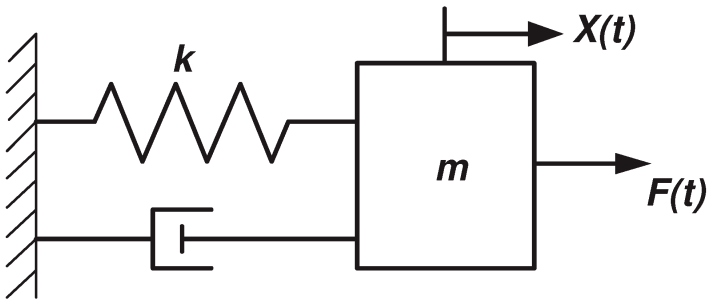

Figure 5.2: Mass-spring model with damper, X(t) in the image is the same as u(t) in the thesis (Gómez-Aguilar et al., 2015)

The equation of motion for this system is given by

$$m\ddot{u}(t) + c\dot{u}(t) + ku(t) = F(t) \tag{5.1}$$

where $u(t)$ is the displacement of the wall at time t, and $F(t)$ is the time-dependent force on the wall, calculated as the dynamic pressure (according to formula 4.1) multiplied by the wall area. The response of the wall is determined numerically using the forward Euler method. In this approach, the acceleration, velocity, and displacement are updated at each time step Δt using the current values. If the displacement exceeds the plastic limit, the spring is considered to have failed and the wall will not return to its original position. The $ku(t)$ term will be replaced by Fpl once $u > Upl$. Fpl is the force found in section 4.4.2. The damping constant c is determined based on the critical damping value, using

$$c = 2\zeta\sqrt{km} \tag{5.2}$$

where ζ is the damping ratio. By plotting the displacement over time, it can be assessed whether Upl or $Ubreak$ is exceeded and if so what the reaction is.

The mass of the wall is determined by first calculating its volume and then accounting for both the concrete and steel reinforcement. The wall has a length of $6.06\,\mathrm{m}$, a thickness of $0.20\,\mathrm{m}$, and a height of $2.59\,\mathrm{m}$, resulting in a total volume of $V_{\text{wall}} = 6.06\,\mathrm{m} \times 0.20\,\mathrm{m} \times 2.59\,\mathrm{m} = 3.14\,\mathrm{m}^3$. Since the wall contains steel reinforcement on both sides with a total steel mass of $141.22\,\mathrm{kg}$, the volume occupied by steel is $V_{\text{steel}} = 141.22\,\mathrm{kg}/7850\,\mathrm{kg/m}^3 = 0.0180\,\mathrm{m}^3$. The remaining volume is occupied by concrete: $V_{\text{concrete}} = 3.14\,\mathrm{m}^3 - 0.0180\,\mathrm{m}^3 = 3.122\,\mathrm{m}^3$. Using a concrete density of $2400\,\mathrm{kg/m}^3$ for C45/55 concrete, the mass of concrete is $7492.82\,\mathrm{kg}$, resulting in a total wall mass of $m = 7492.82\,\mathrm{kg} + 141.22\,\mathrm{kg} = 7634\,\mathrm{kg}$. Not the whole mass moves the whole displacement, different parts can have different displacements. In beams 70% of the mass is used in the mass-spring model. For the wall the same percentage is taken as an assumption. $m = 0.7 \times 7634\,\mathrm{kg} = 5343.8\,\mathrm{kg}$.

The damping coefficient c can now be determined using the calculated mass and the given stiffness k = 16.017.000 N/m. Substituting these values into equation (4.5), and using a typical damping ratio of $\zeta = 0.05$, the damping coefficient is calculated as follows:

$$c = 2 \times 0.05 \times \sqrt{1.6 \times 10^7 \times 5343.8} = 29,300,\mathrm{N\,s/m}$$

This value of c is then used in the dynamic analysis to represent the energy dissipation characteristics of the wall system.

In the appendix the used Python code for the dynamic analysis can be found. The code is based partly on the findings of Janssen (2025), as described in the report ”Schuilplaats onder het Stevin II Lab”.

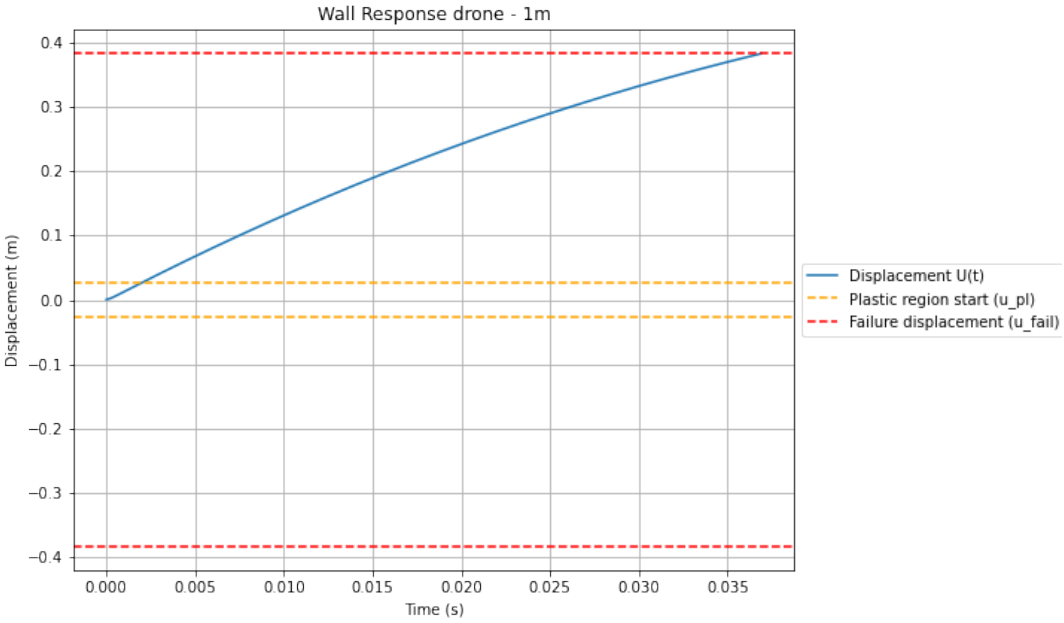

Figure 5.3: Response wall to explosion at 1 meter (Python)

As shown in the figure above, the wall fails when the drone explodes 1 meter away from the structure breaking the reinforcement bars. In Figure 5.2, it may appear that the displacement approaches infinity, but this is not the case. Due to the high load the u is still in the ascending part of the harmonic move.

5.3. Checking the Dynamic Model

5.3.1. Checking the Period

The dynamic model can be validated by comparing its response to that of a free vibration analysis. If the eigen periods are nearly identical, it indicates that the model accurately captures the fundamental dynamic characteristics of the system and is therefore valid to use. This validation is achieved by ensuring purely elastic behavior, which is done by removing plasticity limit. By doing so, the model behaves as a linear elastic system, allowing a direct comparison of natural frequencies and periods without the influence of nonlinear plastic deformation.

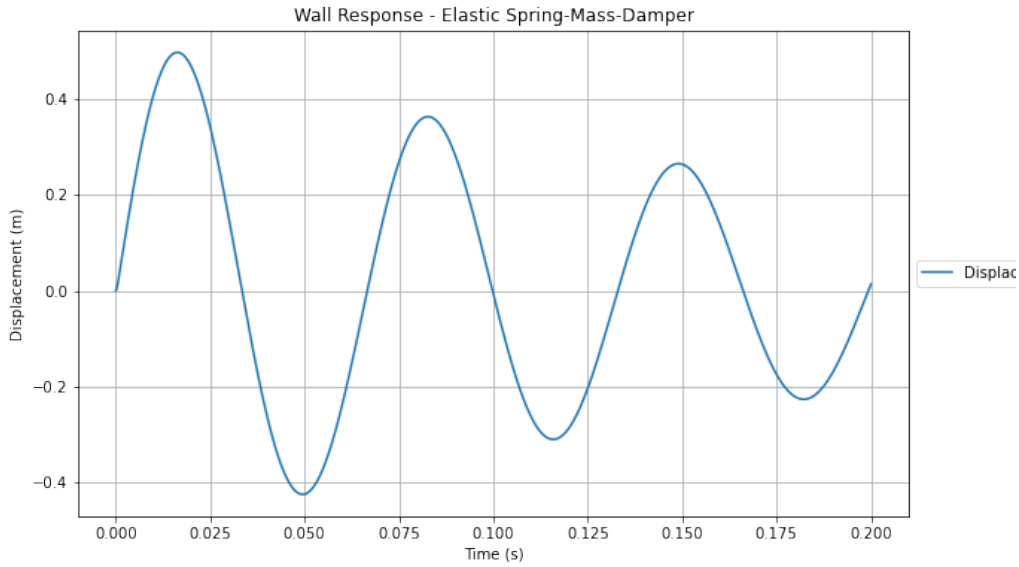

Figure 5.4: Response wall to arbitrairly chosen explosion with elastic spring (Python)

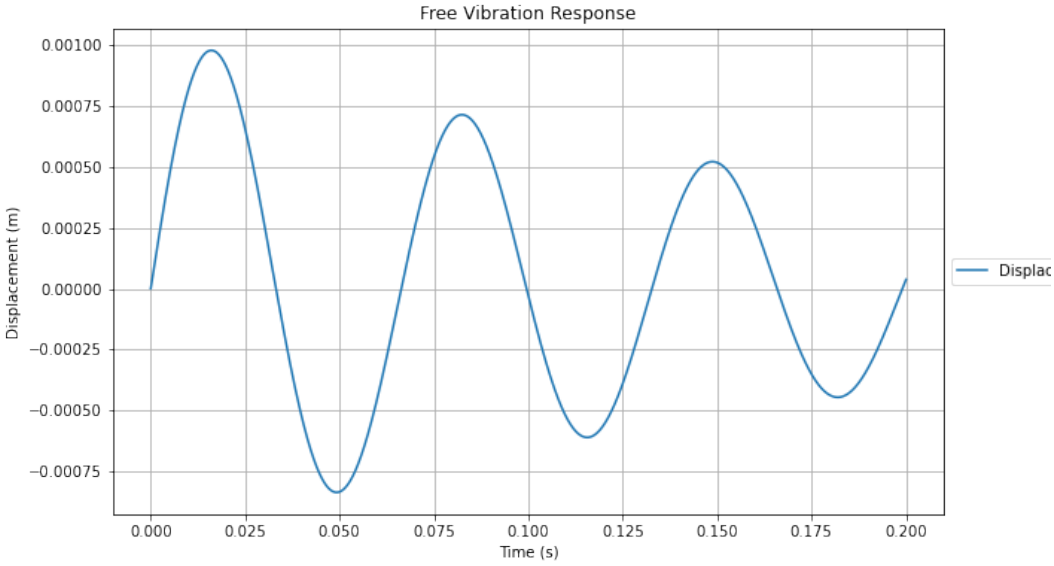

Figure 5.5: Free vibration wall (Python)

$$T = 2\pi\sqrt{\frac{m}{k}} \tag{5.3}$$

where m is the mass and k is the stiffness.

Using:

$$m = 5343.8 \text{ kg}, \quad k = 48050250 \text{ N/m}$$

The eigen period is:

$$T = 2\pi\sqrt{\frac{5343.8}{48050250}} \approx 0.06626 \text{ s}$$

The eigen period calculated manually matches the period obtained from the Python free vibration simulation, which in turn corresponds closely to the period observed in the wall's dynamic response. This consistency confirms that the mass and stiffness are correctly captured in the model.

5.3.2. Influence of Positive Phase Duration and Peak Overpressure

Increasing the positive phase duration t_p and the peak overpressure P_{so} are expected to result in higher displacement amplitudes in the plot.

By comparing the figures below to Figure 5.5, it is evident that doubling either the positive phase duration (t_p) or the peak overpressure (P_{so}), while holding the other variable constant, approximately doubles the displacement.

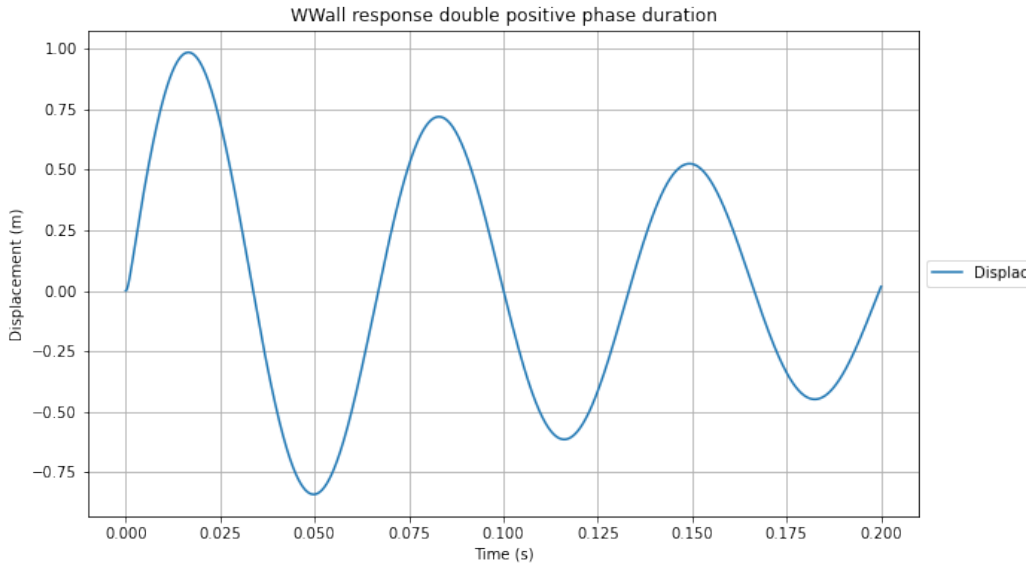

Figure 5.6: Wall response with double positive phase duration (Python)

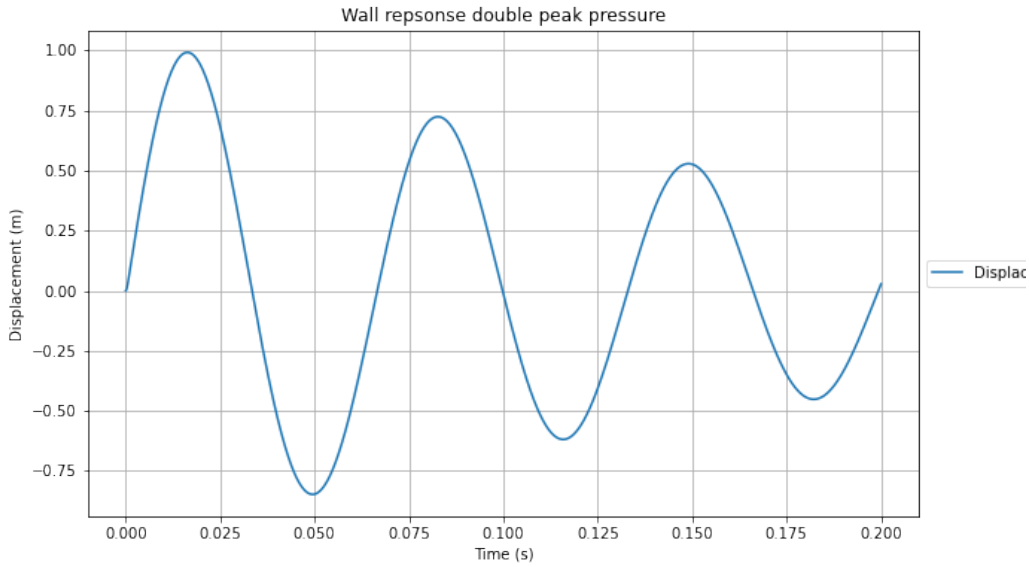

Figure 5.7: Wall response with double peak pressure (Python)

Doubling the positive phase duration roughly doubles the total impulse delivered to the system. Since the displacement is proportional to the energy imparted, the displacement approximately doubles as well. Similarly, doubling the peak overpressure doubles the maximum force applied to the structure. According to Hooke's law, doubling the force results in doubling the displacement. This confirms the correct implementation of t_p and P_{so} in the dynamic model.

5.3.3. Influence of Plastic Spring

To showcase the effect of Upl the Python code is changed and the scenario of plastification of the spring and keeping the spring elastic are plotted in the same diagram.

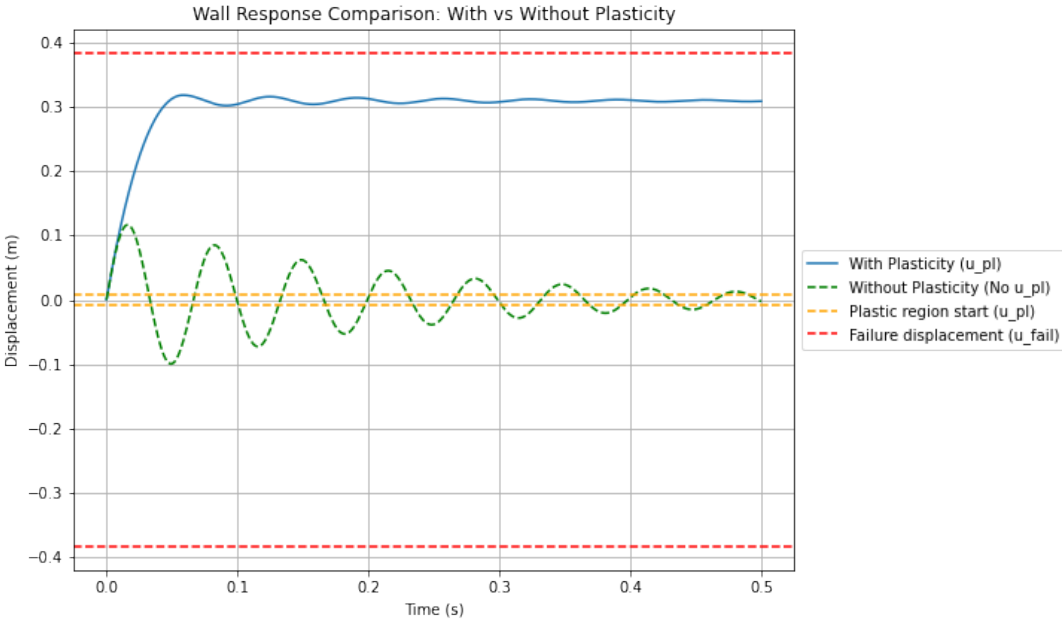

Figure 5.8: Wall response with elastic and plastic spring (Python)

This figure shows what was expected. A linear spring continuously pulls the structure back, as its restoring force is a direct function of displacement, $ku(t)$. For the plastic case, the $ku(t)$ term is replaced with a constant force once the yield displacement is exceeded. Furthermore, the plastic yield displacement (U_{pl}) causes the structure not to return to its original state, thereby validating the use of U_{pl} in the model. The Pyhton codes used for validating the models can be found back in appendix C and D.

6

Shelter Improvement

6.1. Drone Impact on Different Distances

For the impact comparison the following standoff distances from the wall are selected: 1, 2, 5, 10, 20, and 100 meters.

System and Distance (m)	Scaled Distance (Z)	Failure (Yes/No)
Shahed-136 - 1 m	0.684	Yes
Shahed-136 - 2 m	1.37	Yes
Shahed-136 - 5 m	3.42	Yes
Shahed-136 - 10 m	6.84	No
Shahed-136 - 20 m	13.69	No
Shahed-136 - 100 m	68.43	No

Table 6.1: Scaled distances and failure status for Shahed-136 drone at various distances

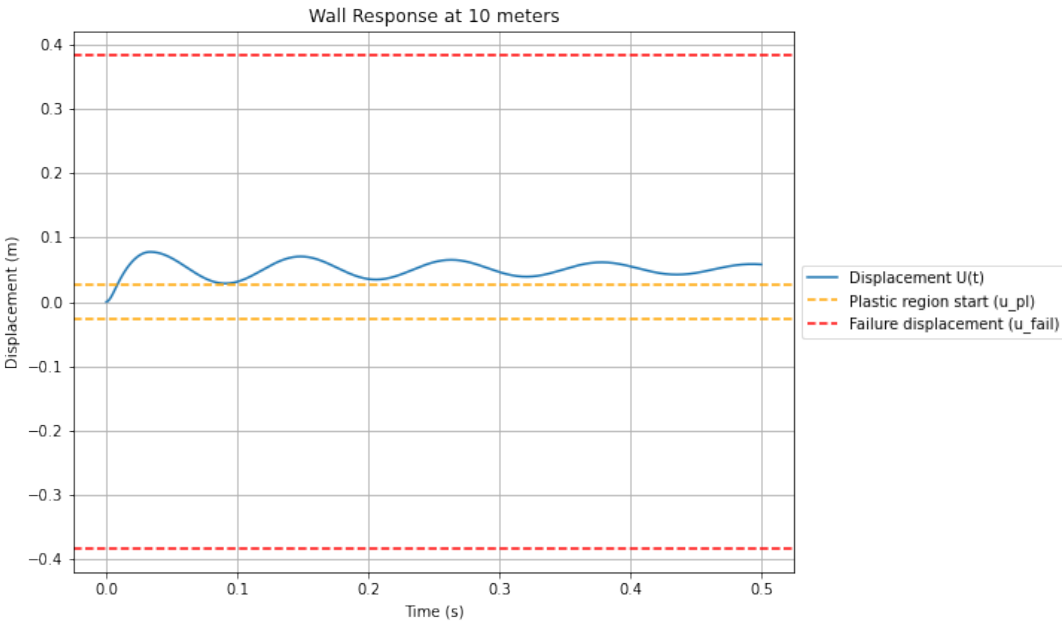

Figure 6.1: Displacement-time curve for Shahed drone at 10 meters distance (Python)

According to Table 6.1 and figure 6.1, the shelter is currently capable of withstanding an explosion

occurring at a distance of 10 meters or more. However, if the explosion occurs closer than 10 meters to the shelter wall, the wall will fail. In the next sections possible reinforcement options are researches to see if the performance of the shelter can be enhances.

6.2. Reinforcement Placement

The next sections investigate possible reinforcement options to assess improvements in the shelter's performance. In the initial design, the reinforcement was placed at the mid-depth of the wall, which is structurally inefficient. By positioning the reinforcement closer to the tension zone, the effective lever arm is increased, thereby enhancing the plastic moment capacity of the section.

If reinforcement is moved to the tension side and keeping a coverage of 25 mm, the effective lever arm is:

$$d = c + \frac{\phi}{2} = 25 + 6 = 31 \text{ mm}, \quad z = t - d = 200 - 31 = 169 \text{ mm} = 0.169 \text{ m}$$

Plastic moment capacity:

$$m_p = A_{s,1m} \cdot f_{yd} \cdot z = 0.00065 \cdot 435 \times 10^6 \cdot 0.169 \approx 41.6 \text{ kNm/m}$$

Failure load:

$$w_u = \frac{72}{5} \cdot \frac{m_p}{a^2} = 14.4 \cdot \frac{41,600}{2.59^2} \approx 89.4 \text{ kPa}$$

Since the reinforcement bars are now placed in a normal location of the tension zone one third of the E-modulus can be used for the cracked concrete. Plugging this load into SCIA and performing an elastic analysis the displacement becomes: 1.8 mm. Multiplying this by 3 to take into account the concrete has cracked gives u = 5.4 mm.

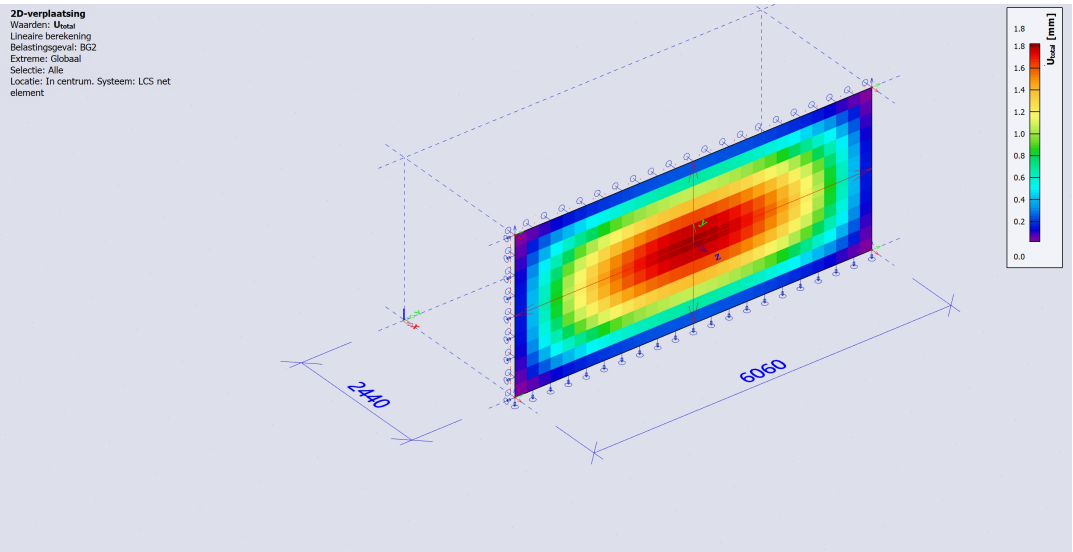

Figure 6.2: Deflection under a load of 89.4 KPa (Python)

Using the same method as in section 4.3, the stiffness is: 127,324.57 KN/m.

6.3. Ground Layer

One way to enhance the strength of the shelter is by adding a layer of clay in front of the wall. This additional mass acts as an additional mass in the mass-spring system, improving the structure's ability to absorb and dissipate forces. Beyond increasing strength, this clay layer plays a crucial role in camouflage, helping the shelter blend into its surroundings and reducing the risk of detection.

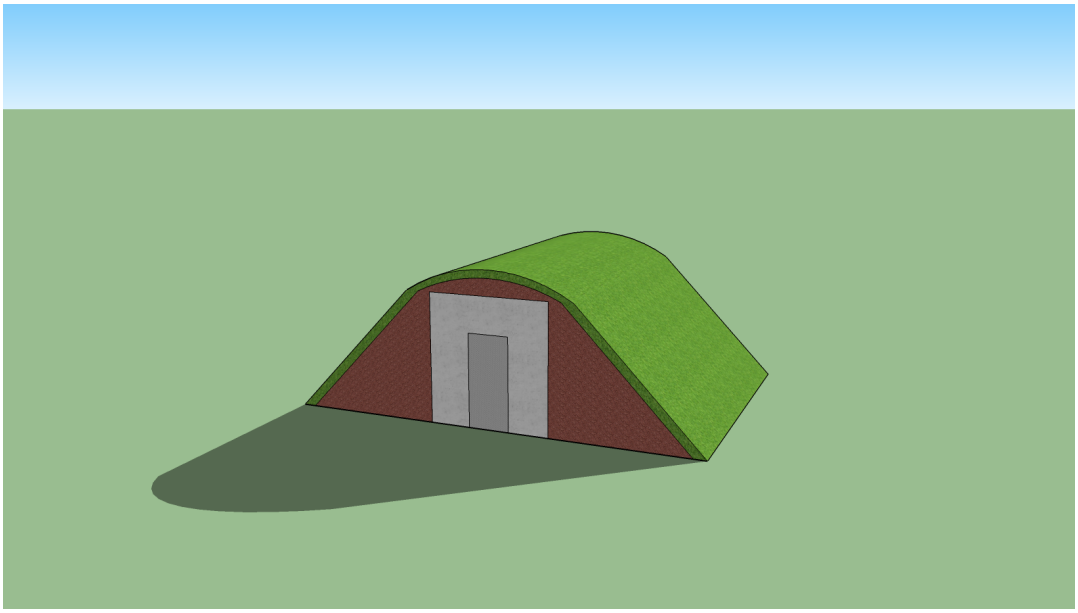

Figure 6.3: Shelter design with clay layer (Sketchup)

Besides the strength this will also deliver an extra force to the wall which needs to be calculated.

To get a stable clay slope, an angle of 30 degrees is chosen. First there is a rectangular section with a depth of 0.5 meters. after that the slope starts. the height is 2.59 meters meaning the depth of the wedge is 4.46 meters, rounded of the 4.5 meters. It is assumed that 30% of the mass will actually move and is taken as an extra mass in the dynamic model. Besides being an extra mass the horizontal pressure needs to be added as a static pressure in the dynamic model.

Rectangular volume:

$$\begin{aligned} V_{\text{rect}} &= H \cdot b_{\text{rect}} \cdot L \\ &= 2.59 \cdot 0.5 \cdot 6.06 \\ &\approx 7.84\,\text{m}^3 \end{aligned}$$

Triangular volume:

$$\begin{aligned} V_{\text{tri}} &= \tfrac{1}{2} \cdot H \cdot b_{\text{tri}} \cdot L \\ &= 0.5 \cdot 2.59 \cdot 3.0 \cdot 6.06 \\ &\approx 23.56\,\text{m}^3 \end{aligned}$$

Total soil wedge volume:

$$\begin{aligned} V_{\text{total}} &= V_{\text{rect}} + V_{\text{tri}} \\ &= 7.84 + 23.56 \\ &= 31.40\,\text{m}^3 \end{aligned}$$

Total soil mass:

$$\begin{aligned} m_{\text{soil,total}} &= \frac{V_{\text{total}} \cdot \gamma}{g} \\ &= \frac{31.40 \cdot 20{,}000}{9.81} \\ &\approx 64{,}016\,\text{kg} \end{aligned}$$

Effective moving mass (30%):

$$\begin{aligned} m_{\text{soil,eff}} &= k_{\text{eff}} \cdot m_{\text{soil,total}} \\ &= 0.30 \cdot 64{,}016 \\ &\approx 19{,}205\,\text{kg} \end{aligned}$$

Horizontal stress at base:

$$\begin{aligned} \sigma_{h,\text{base}} &= K_0 \cdot \gamma \cdot H \\ &= 0.5 \cdot 20{,}000 \cdot 2.59 \\ &\approx 25{,}900\,\text{N/m}^2 \\ &= 25.9\,\text{kPa} \end{aligned}$$

Resultant force per unit length (triangular distribution):

$$\begin{aligned} F' &= \tfrac{1}{2} \cdot \sigma_{h,\text{base}} \cdot H \\ &= 0.5 \cdot 25{,}900 \cdot 2.59 \\ &\approx 33{,}500\,\text{N/m} \end{aligned}$$

Total thrust on wall:

$$\begin{aligned} F_{\text{static}} &= F' \cdot L \\ &= 33{,}500 \cdot 6.06 \\ &\approx 203{,}000\,\text{N} \\ &\approx 203\,\text{kN} \end{aligned}$$

This force is put as a constant in the dynamic analysis.

Besides acting as additional mass in the mass-spring model, the soil will also reduce the overpressure with which the explosion impacts the wall. Considering a hemispherical blast, the closest distance from the explosion source to the center of the wall is calculated as 0.5+0.5×4.5=2.75 meters. This means that the effective distance between the explosion and the wall increases initially, which alone contributes to a reduction in blast intensity.

Moreover, the propagation of the blast wave through soil differs significantly from that in air. Soil, being a denser and more heterogeneous medium, attenuates the blast wave more rapidly due to energy absorption. As the blast wave travels through the soil, its peak pressure decreases and the positive phase duration typically lengthens due to the slower wave speed. This results in a lower and more prolonged pressure load reaching the wall compared to a blast traveling solely through air.

In this analysis, the attenuation of the blast waves in the soil is neglected, which causes the force impacting the structure to be overestimated. This conservative assumption will likely lead to over dimensioning of the structure, but does not compromise safety.

6.4. Improvement Results on Drone Impact

By applying these improvements, the following displacement-time graph is obtained. It illustrates an explosion occurring 2.75 meters from the wall through air. While modeling the explosion through air is a simplification, this approach demonstrates that despite the increased mass, greater distance, and repositioning of the reinforcement, the wall still fails under these conditions. The python code can be found in appendix B.

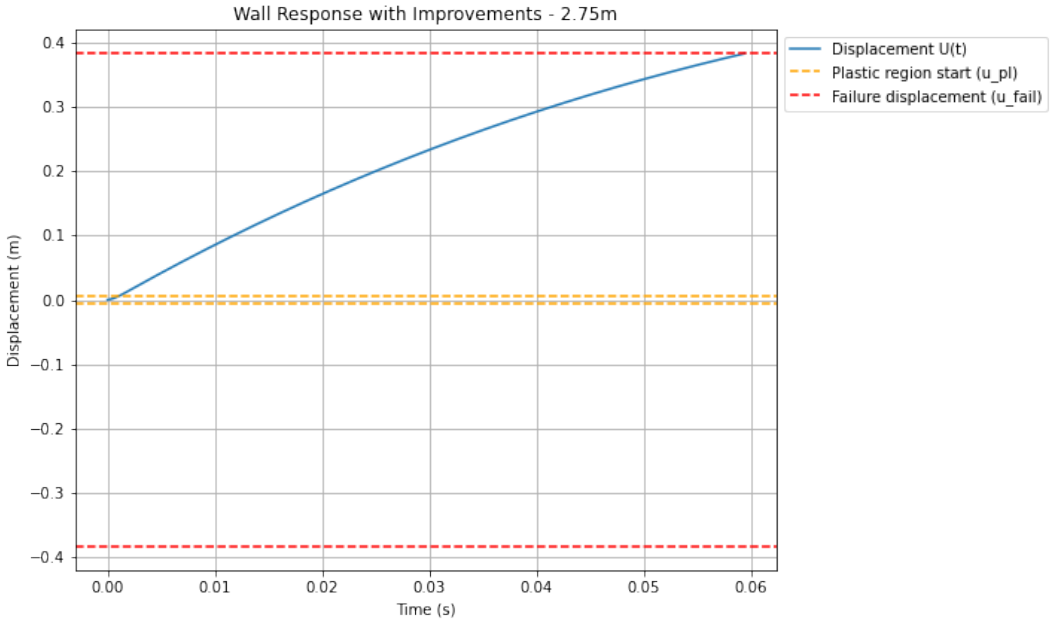

Figure 6.4: Displacement-time diagram for explosion at the soil layer (Pyhton)

Applying the same model to a distance of 5 meter gives the following figure:

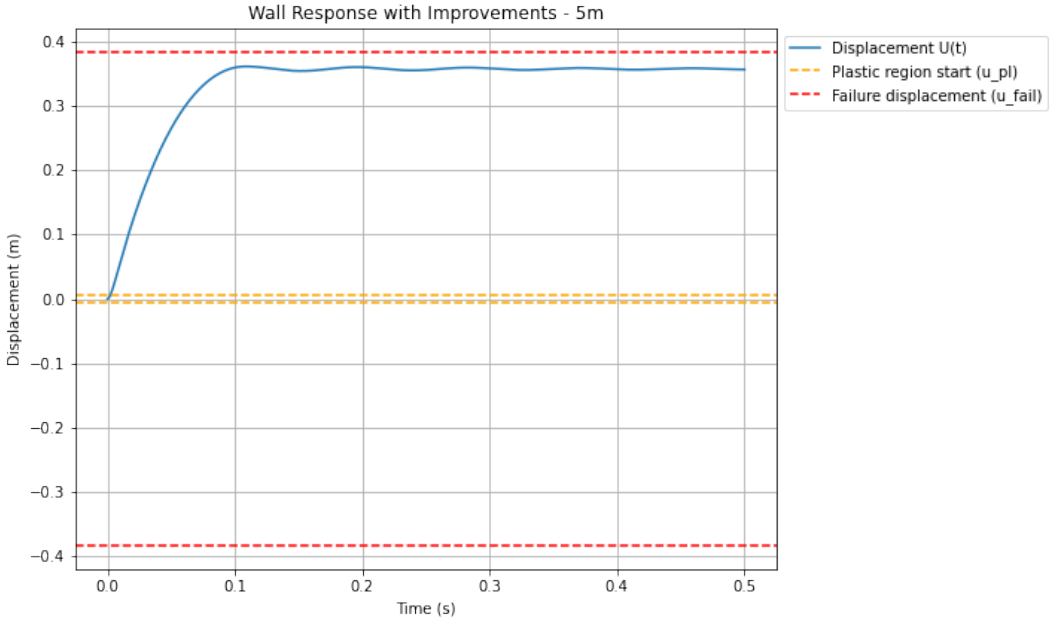

Figure 6.5: Displacement-time diagram for explosion at 2.25 meters from the soil layer (Pyhton)

6.4.1. Results with Other Explosives

Using Figure 5.1 and Formula 2.2, the relevant blast parameters are determined for some other explosives. These parameters are then put into the dynamic response code to evaluate structural performance and identify any potential failures. The scaled distances are applied to three representative explosive systems selected based on their relative explosive power. The Shahab-3, being the most powerful missile in the set, represents the upper bound of blast effects and structural threat. The Tochka-U, as the strongest among the medium-power rockets, is analyzed accordingly. The 155 mm

HE Artillery Grenade is included for analysis to assess its effects relative to the drone case, despite its smaller explosive charge. In this analysis, the attenuation of the pressure due to the soil is again neglected. The corresponding response diagrams, including all displacement-time curves up to the first distance at which no further failure occurs, are provided in Appendix E. The analysis starts at 2.75 m since this is the closest distance to the wall the explosion can occur due to the soil placement.

Case	Scaled Distance	Failure
Shahab-3 - 2.75 m	0.65	Yes
Shahab-3 - 5 m	1.19	Yes
Shahab-3 - 10 m	2.37	Yes
Shahab-3 - 20 m	4.74	No
Shahab-3 - 100 m	23.72	No
Tochka-U - 2.75 m	0.88	Yes
Tochka-U - 5 m	1.61	Yes
Tochka-U - 10 m	6.11	No
Tochka-U - 20 m	6.43	No
Tochka-U - 100 m	32.15	No
155 mm HE Artillery Grenade - 2.75 m	3.77	Yes
155 mm HE Artillery Grenade - 5 m	-	No
155 mm HE Artillery Grenade - 10 m	-	No
155 mm HE Artillery Grenade - 20 m	-	No
155 mm HE Artillery Grenade - 100 m	-	No

Table 6.2: Failure assessment across explosives and stand-off distances.

7

Discussion

The dynamic model gives consistent results and captures the main behaviors well. With a 200 mm wall, limited resistance to very large blasts is expected. Moving the reinforcement to the tension zone and adding a soil layer increases strength as predicted.

When the initial overpressure is very high, for example when a Shabab missile at close range strikes, the response curves show a fast rise in displacement up to Upl. The straight, flat segment above this point indicates plastification. The restoring force stops growing with displacement and stays at a constant plastic level. After yielding, the system can still move and show oscillations. If the blast is very strong, the constant plastic force is not enough to stop the motion before it reaches $Ubreak$. Increasing the distance (larger scaled distance z) rapidly reduces peak overpressure, so the wall response becomes less severe and this runaway behavior fades. This shows that increasing the standoff distance has a nonlinear effect on the structure's response. Therefore, in addition to structural strength, impact distance is an important variable to manage.

Throughout the thesis multiple assumptions have been made. Although most of these assumptions had an explanation this can still impact the accuracy of the results. Besides that, the accuracy can also have decreased by the precision in which the explosive blasts parameters are depicted in the design graph. Due to the big scale accurate reading is difficult.

One key simplification is treating wave travel in soil the same as in air. In reality, soil tends to attenuate the blast and shorten the pressure pulse, likely reducing peaks at the wall. This means the real shelter may perform a bit better than the model suggests. On the other hand, potentially harmful effects were also not modeled, such as a direct drone impact. If a drone buries itself in the soil layer, it reduces the standoff distance to the wall and adds additional kinetic forces.

The results should be interpreted as an initial indication of the robustness of prefabricated shelter walls, providing a sense of what can be expected when a wall is subjected to explosive blasts. They are best used to compare design options and identify key drivers rather than to define exact capacity limits.

It would be interesting to see what it would take to make the shelter wall able to resist drone impacts at a distance of 2.75 meters. Increasing the wall thickness could be an option, but due to time span of the thesis not researched.

8

Conclusion

Prefabricated concrete shelters can provide protection against modern explosive threats. Because direct-impact modeling is costly and not economically feasible for routine design, the primary objective for civilian shelters is to mitigate blast shock waves. A shelter with the dimensions of a 20-ft shipping container facilitates easy transport and rapid deployment.

An unreinforced wall does not provide sufficient protection so reinforcement is required. Placing B500B steel in the tension zone and adding a soil layer to increase the mass and help energy absorption will significantly improve the performance. Based on the analyses, the upgraded shelter is expected to withstand artillery shells at any practical standoff distance, resist drone detonations from about 5 meters and beyond, provide protection against medium ballistic missiles from roughly 10 meters, and offer protection against higher-yield ballistic missiles from around 20 meters. These thresholds are approximates but do show the potential that prefabricated shelters can offer in times of war. Before advancing this design, further research with more advanced models is required.

Bibliography

[1] Anas, S. M., & Alam, M. (2021). Comparison of Existing Empirical Equations for Blast Peak Positive Overpressure from Spherical Free Air and Hemispherical Surface Bursts. *Iranian Journal of Science and Technology Transactions of Civil Engineering, 46*(2), 965–984. https://doi.org/10.1007/s40996-021-00718-4

[2] Axe, D. (2025, March 12). 4.5 million drones is a lot of drones. It's Ukraine's new production target for 2025. *Forbes*. https://www.forbes.com/sites/davidaxe/2025/03/12/45-million-drones-is-a-lot-of-drones-its-ukraines-new-production-target-for-2025/

[3] Blaauwendraad, J. (2016). *Dynamica van systemen: CTB2300 collegedictaat* (Jan 2016 ed.). Technische Universiteit Delft, Faculteit Civiele Techniek en Geowetenschappen, Afdeling Mechanica, Materialen en Constructies.

[4] Catovic, A., & Kljuno, E. (2021). Comparation of Analytical Models and Review of Numerical Simulation Method for Blast Wave Overpressure Estimation after the Explosion. https://www.researchgate.net/publication/349109974_Comparation_of_Analytical_Models_and_Review_of_Numerical_Simulation_Method_for_Blast_Wave_Overpressure_Estimation_after_the_Explosion

[5] Dahlgren, M. (2024a, April 23). KH-47M2 Kinzhal | Missile Threat. *Missile Threat*. https://missilethreat.csis.org/missile/kinzhal/

[6] Dahlgren, M. (2024b, April 23). Tomahawk | Missile Threat. *Missile Threat*. https://missilethreat.csis.org/missile/tomahawk/

[7] Draganić, H., & Sigmund, V. Z. (n.d.). Blast Loading on Structures. https://www.researchgate.net/publication/273659070_Blast_Loading_on_Structures

[8] EU Debates, eudebates.tv. (2024, December 13). We are not at war - But we are certainly not at peace either! NATO Chief [Video]. *YouTube*. https://www.youtube.com/watch?v=TBlvDv5ut7U

[9] Filice, A., Mynarz, M., & Zinno, R. (2022). Experimental and Empirical Study for Prediction of Blast Loads. *Applied Sciences, 12*(5), 2691. https://doi.org/10.3390/app12052691

[10] Gluck, M. (2024, April 23). 9K720 Iskander (SS-26) | Missile Threat. *Missile Threat*. https://missilethreat.csis.org/missile/ss-26-2/

[11] Gómez-Aguilar, J., Yépez-Martínez, H., Calderón-Ramón, C., Cruz-Orduña, I., Escobar-Jiménez, R., & Olivares-Peregrino, V. (2015). Modeling of a Mass-Spring-Damper System by Fractional Derivatives with and without a Singular Kernel. *Entropy*, 17(9), 6289–6303. https://doi.org/10.3390/e17096289

[12] Jeon, D., Kim, K., & Han, S. (2017). Modified equation of shock wave parameters. *Computation, 5*(3), 41. https://doi.org/10.3390/computation5030041

[13] Janssen, J. (2025). Schuilplaats onder het Stevin II lab: Een onderzoek naar de weerstand van de vloer van het Stevin II laboratorium tegen explosieven. *Bachelor's thesis, Technische Universiteit Delft*. https://phoogenboom.nl/BSc_projects/eindrapport_janssen.pdf

[14] Kingery, C. N., & Bulmash, G. (1984). Airblast Parameters from TNT Spherical Air Burst and Hemispherical Surface Burst; Technical Report ARBRL-TR-02555; U.S. Army BRL: Aberdeen Proving Ground, MD, USA.

[15] Kinney, G. F., & Graham, K. J. (1985). Explosive shocks in air. In *Springer eBooks*. https://doi.org/10.1007/978-3-642-86682-1

[16] NatStrat. (2021, April 22). The evolution of modern warfare: How technology is transforming the rules of war. https://www.natstrat.org/articledetail/publications/the-evolution-of-modern-warfare-how-technology-is-transforming-the-rules-of-war-212.html

[17] NOS Nieuws. (2024, November 26). Nederland heeft geen schuilkelders en dat blijft voorlopig zo. *NOS*. https://nos.nl/artikel/2546039-nederland-heeft-geen-schuilkelders-en-dat-blijft-voorlopig-zo

[18] Panait, C. (2024). The evolution of aerial threats and their implications on army operations. *Revista Academiei Forțelor Terestre, 29*(4), 481–488. https://doi.org/10.2478/raft-2024-0050

[19] Shaikh, S. (2024a, April 23). OTR-21 Tochka (SS-21) | Missile Threat. *Missile Threat*. https://missilethreat.csis.org/missile/ss-21/

[20] Shaikh, S. (2024b, April 23). Shahab-3 | Missile Threat. *Missile Threat*. https://missilethreat.csis.org/missile/shahab-3/

[21] Trajkovski, J., Kunc, R., Perenda, J., & Prebil, I. (2014). Minimum mesh design criteria for blast wave development and structural response - MMALE method. *Latin American Journal of Solids and Structures, 11*(11), 1999–2017. https://doi.org/10.1590/s1679-78252014001100006

[22] Vrouwenvelder, A. C. W. M., & Witteveen, J. (2003). *The plastic behaviour and the calculation of plates subjected to bending*. Technical University Delft, Faculty of Civil Engineering and Geosciences.

[23] Wikipedia contributors. (2025b, June 27). Ballistic missile. *Wikipedia*. https://en.wikipedia.org/wiki/Ballistic_missile

[24] Wikipedia contributors. (2025e, July 6). Cruise missile. *Wikipedia*. https://en.wikipedia.org/wiki/Cruise_missile

[25] Wikipedia contributors. (2025c, June 27). Hypersonic weapon. *Wikipedia*. https://en.wikipedia.org/wiki/Hypersonic_weapon

[26] Wikipedia contributors. (2025d, June 28). HESA Shahed 136. *Wikipedia*. https://en.wikipedia.org/wiki/HESA_Shahed_136

[27] Wikipedia contributors. (2025a, May 29). BM-30 Smerch. *Wikipedia*. https://en.wikipedia.org/wiki/BM-30_Smerch

A

Python Code Dynamic Response

```python
import numpy as np
import matplotlib.pyplot as plt

# --- Explosion Parameters ---
P_so = 13099038      # peak overpressure (Pa)
t_p = 0.00086         # positive phase duration (s)
b = 1.0                  # waveform parameter

# --- Wall / Structure Parameters ---
A = 6.06 * 2.59          # wall area (m^2)
Fp_pressure = 52300      # plastic force pressure (Pa, 52.3 kPa)
k_elastisch = 16016666 # spring constant (N/m)
m_muur = 5343.8           # wall mass (kg)
u_pl = 0.0264           # plastic region yield displacement (m)
u_fail = 0.382           # failure displacement (m)

# Derived parameters
Fp = Fp_pressure * A     # constant plastic force (N)

# Damping function (Rayleigh critical ratio)
def damping(m, k, zeta=0.05):
    return 2 * zeta * np.sqrt(k * m)

c = damping(m_muur, k_elastisch)
# Overpressure function
def delta_P(t):
    if t < 0 or t > t_p:
        return 0
    return P_so * (1 - t / t_p) * np.exp(-b * t / t_p)

# Euler integration with plastic memory
def Euler(t_max, dt):
    t_list, u_list = [], []
    v = 0.0
    u = 0.0
    u_plastic = 0.0   # plastic offset memory
    t = 0.0

    while t < t_max:
        # External forcing
        P = delta_P(t)
        F = P * A

        # Internal restoring force with plasticity
        u_elastic = u - u_plastic
        if abs(u_elastic) < u_pl:
            spring_force = k_elastisch * u_elastic
        else:
            # Plastic yielding - cap force, shift plastic offset
```

```
            spring_force = np.sign(u_elastic) * Fp
            u_plastic = u - np.sign(u_elastic) * u_pl

        # Equation of motion
        a = (F - c * v - spring_force) / m_muur
        v = v + dt * a
        u = u + dt * v

        t_list.append(t)
        u_list.append(u)

        # Stop if failure displacement reached
        if abs(u) >= u_fail:
            print(f"Failure at t = {t:.6f} s, u = {u:.6f} m")
            break

        t += dt

    return t_list, u_list

# --- Simulation parameters ---
t_max = 0.5
dt = 1.0e-4

# Run simulation
t_list, u_list = Euler(t_max, dt)

# Plotting
plt.figure(figsize=(10,6))
plt.plot(t_list, u_list, label='Displacement U(t)')
plt.axhline(u_pl, color='orange', linestyle='--', label='Plastic region start (u_pl)')
plt.axhline(-u_pl, color='orange', linestyle='--')
plt.axhline(u_fail, color='red', linestyle='--', label='Failure displacement (u_fail)')
plt.axhline(-u_fail, color='red', linestyle='--')
plt.xlabel('Time (s)')
plt.ylabel('Displacement (m)')
plt.title('Wall Response')
plt.grid()


plt.legend(loc='center left', bbox_to_anchor=(1, 0.5))
plt.tight_layout()
plt.subplots_adjust(right=0.75)
plt.show()
```

B

Python Code Dynamic Response with Improvements

```python
import numpy as np
import matplotlib.pyplot as plt

# --- Explosion Parameters ---
P_so = 17236893       # peak overpressure (Pa)
t_p = 0.0022         # positive phase duration (s)
b = 1.0                  # waveform parameter

# --- Wall / Structure Parameters ---
k_elastisch = 127324572  # spring constant (N/m)
m_muur = 5343.8            # wall mass (kg)
m_soil_eff = 19205       # effective soil mass (kg) - 30% of clay wedge
m_effective = m_muur + m_soil_eff  # total effective mass (kg)
F_static = 203000        # static earth pressure force (N)
u_pl = 0.0054           # plastic region yield displacement (m)
u_fail = 0.382           # failure displacement (m)
A = 6.06 * 2.59          # wall area (m^2)
Fp_pressure = 89400      # plastic force pressure (Pa, 52.3 kPa)

# Derived parameters
Fp = Fp_pressure * A     # constant plastic force (N)

# Damping function (Rayleigh critical ratio)
def damping(m, k, zeta=0.05):
    return 2 * zeta * np.sqrt(k * m)

c = damping(m_effective, k_elastisch)

# Overpressure function
def delta_P(t):
    if t < 0 or t > t_p:
        return 0
    return P_so * (1 - t / t_p) * np.exp(-b * t / t_p)

# Euler integration with plastic memory
def Euler(t_max, dt):
    t_list, u_list = [], []
    v = 0.0
    u = 0.0
    u_plastic = 0.0   # plastic offset memory
    t = 0.0

    while t < t_max:
        # External forcing
        P = delta_P(t)
        F = P * A + F_static  # blast pressure + static earth pressure
```

```
47
48          # Internal restoring force with plasticity
49          u_elastic = u - u_plastic
50          if abs(u_elastic) < u_pl:
51              spring_force = k_elastisch * u_elastic
52          else:
53              # Plastic yielding - cap force, shift plastic offset
54              spring_force = np.sign(u_elastic) * Fp
55              u_plastic = u - np.sign(u_elastic) * u_pl
56
57          # Equation of motion
58          a = (F - c * v - spring_force) / m_effective
59          v = v + dt * a
60          u = u + dt * v
61
62          t_list.append(t)
63          u_list.append(u)
64
65          # Stop if failure displacement reached
66          if abs(u) >= u_fail:
67              print(f"Failure at t = {t:.6f} s, u = {u:.6f} m")
68              break
69
70          t += dt
71
72      return t_list, u_list
73
74  # --- Simulation parameters ---
75  t_max = 0.5
76  dt = 1.0e-4
77
78  # Run simulation
79  t_list, u_list = Euler(t_max, dt)
80
81  # Plotting
82  plt.figure(figsize=(10,6))
83  plt.plot(t_list, u_list, label='Displacement U(t)')
84  plt.axhline(u_pl, color='orange', linestyle='--', label='Plastic region start (u_pl)')
85  plt.axhline(-u_pl, color='orange', linestyle='--')
86  plt.axhline(u_fail, color='red', linestyle='--', label='Failure displacement (u_fail)')
87  plt.axhline(-u_fail, color='red', linestyle='--')
88  plt.xlabel('Time (s)')
89  plt.ylabel('Displacement (m)')
90  plt.title('Wall Response with Improvements - 2.75m')
91  plt.grid()
92  plt.legend(loc='upper left', bbox_to_anchor=(1, 1))
93  plt.tight_layout()
94  plt.show()
```

C

Wall Response - Elastic Spring-Mass-Damper

```python
import numpy as np
import matplotlib.pyplot as plt
from scipy.signal import find_peaks

# --- Explosion Parameters ---
P_so = 48263320         # peak overpressure (Pa)
t_p = 0.00096           # positive phase duration (s)

# --- Wall / Structure Parameters ---
b = 1.0                  # waveform parameter
A = 6.06 * 2.59          # wall area (m^2)

k_elastisch = 48050250  # spring constant (N/m)
m_muur = 5343.8         # wall mass (kg)

# Damping function (Rayleigh critical ratio)
def damping(m, k, zeta=0.05):
    return 2 * zeta * np.sqrt(k * m)

c = damping(m_muur, k_elastisch, zeta=0.05)  # 5% damping

# Overpressure function
def delta_P(t):
    if t < 0 or t > t_p:
        return 0
    return P_so * (1 - t / t_p) * np.exp(-b * t / t_p)

# Euler integration without plasticity or failure
# Pure elastic spring-mass-damper system

def Euler_elastic(t_max, dt):
    t_list, u_list = [], []
    v = 0.0
    u = 0.0
    t = 0.0

    while t < t_max:
        # External forcing
        P = delta_P(t)
        F = P * A

        # Elastic spring force
        spring_force = k_elastisch * u

        # Equation of motion
        a = (F - c * v - spring_force) / m_muur
```

```
        v = v + dt * a
        u = u + dt * v

        t_list.append(t)
        u_list.append(u)

        t += dt

    return np.array(t_list), np.array(u_list)

# --- Simulation parameters ---
t_max = 0.2  # short time to capture vibration
dt = 1.0e-5

# Run simulation

t_list, u_list = Euler_elastic(t_max, dt)

# Find peaks in displacement to calculate period
peaks, _ = find_peaks(u_list)
peak_times = t_list[peaks]

if len(peak_times) > 1:
    periods = np.diff(peak_times)
    simulated_period = np.mean(periods)
    print(f"Simulated period: {simulated_period:.8f} s")
else:
    simulated_period = None
    print("Not enough peaks to calculate period.")

# Theoretical natural period
omega_n = np.sqrt(k_elastisch / m_muur)
T_n = 2 * np.pi / omega_n
print(f"Theoretical natural period: {T_n:.8f} s")

# Plotting
plt.figure(figsize=(10,6))
plt.plot(t_list, u_list, label='Displacement U(t)')
plt.xlabel('Time (s)')
plt.ylabel('Displacement (m)')
plt.title('Wall Response - Elastic Spring-Mass-Damper')
plt.grid()
plt.legend(loc='center left', bbox_to_anchor=(1, 0.5))
plt.savefig("Wall-elastic response.png")
plt.show()
```

Free vibration:

```
import numpy as np
import matplotlib.pyplot as plt
from scipy.signal import find_peaks

# Parameters
k_elastisch = k_elastisch # spring constant (N/m)
m_muur = m_muur          # wall mass (kg)
zeta = 0.05              # damping ratio

# Calculate theoretical natural frequency and period
omega_0 = np.sqrt(k_elastisch / m_muur)
T_theoretical = 2 * np.pi / omega_0
print(f"Theoretical natural frequency (rad/s): {omega_0:.2f}")
print(f"Theoretical period (s): {T_theoretical:.5f}")

# Damping coefficient
c = 2 * zeta * np.sqrt(k_elastisch * m_muur)

# Free vibration simulation parameters
t_max = 0.2
dt = 1e-5
n_steps = int(t_max / dt)

```

```
# Initial conditions
u = 0.0  # initial displacement (m)
v = 0.1   # initial velocity (m/s)

# Lists to store results
t_list = []
u_list = []

for i in range(n_steps):
    t = i * dt
    # No external force
    F_ext = 0.0

    # Spring force (linear elastic)
    F_spring = -k_elastisch * u

    # Damping force
    F_damping = -c * v

    # Acceleration
    a = (F_ext + F_spring + F_damping) / m_muur

    # Euler integration
    v += a * dt
    u += v * dt

    t_list.append(t)
    u_list.append(u)

# Find peaks to calculate period
peaks, _ = find_peaks(u_list)
peak_times = np.array(t_list)[peaks]

# Calculate periods between peaks
periods = np.diff(peak_times)
T_simulated = np.mean(periods)

print(f"Simulated period (s): {T_simulated:.5f}")

# Plot displacement
plt.figure(figsize=(10,6))
plt.plot(t_list, u_list, label='Displacement (free vibration)')
plt.xlabel('Time (s)')
plt.ylabel('Displacement (m)')
plt.title('Free Vibration Response')
plt.grid()
plt.legend(loc='center left', bbox_to_anchor=(1, 0.5))
plt.savefig("Wall_freevib.png")
plt.show()
```

D

Python Code With vs Without Plasticity

```python
#showcasing plasticity
import numpy as np
import matplotlib.pyplot as plt

# --- Explosion Parameters ---
P_so = 10000000        # peak overpressure (Pa)
t_p = 0.00096           # positive phase duration (s)

# --- Wall / Structure Parameters ---
b = 1.0                  # waveform parameter
A = 6.06 * 2.59          # wall area (m^2)
Fp_pressure = 52300      # plastic force pressure (Pa, 52.3 kPa)
k_elastisch = 48050250   # spring constant (N/m)
m_muur = 5343.8          # wall mass (kg)
u_pl = 0.0088            # plastic region yield displacement (m)
u_fail = 0.382           # failure displacement (m)

# Derived parameters
Fp = Fp_pressure * A     # constant plastic force (N)

# Damping function (Rayleigh critical ratio)
def damping(m, k, zeta=0.05):
    return 2 * zeta * np.sqrt(k * m)

c = damping(m_muur, k_elastisch)

# Overpressure function
def delta_P(t):
    if t < 0 or t > t_p:
        return 0
    return P_so * (1 - t / t_p) * np.exp(-b * t / t_p)

# Euler integration with plastic memory (original)
def Euler_with_plastic(t_max, dt):
    t_list, u_list = [], []
    v = 0.0
    u = 0.0
    u_plastic = 0.0   # plastic offset memory
    t = 0.0

    while t < t_max:
        P = delta_P(t)
        F = P * A

        u_elastic = u - u_plastic
        if abs(u_elastic) < u_pl:
```

```
            spring_force = k_elastisch * u_elastic
        else:
            spring_force = np.sign(u_elastic) * Fp
            u_plastic = u - np.sign(u_elastic) * u_pl

        a = (F - c * v - spring_force) / m_muur
        v = v + dt * a
        u = u + dt * v

        t_list.append(t)
        u_list.append(u)

        if abs(u) >= u_fail:
            print(f"Failure with plasticity at t = {t:.6f} s, u = {u:.6f} m")
            break

        t += dt

    return t_list, u_list

# Euler integration without plastic memory (no u_pl)
def Euler_without_plastic(t_max, dt):
    t_list, u_list = [], []
    v = 0.0
    u = 0.0
    t = 0.0

    while t < t_max:
        P = delta_P(t)
        F = P * A

        # Purely elastic spring force, no plastic offset
        spring_force = k_elastisch * u

        a = (F - c * v - spring_force) / m_muur
        v = v + dt * a
        u = u + dt * v

        t_list.append(t)
        u_list.append(u)

        if abs(u) >= u_fail:
            print(f"Failure without plasticity at t = {t:.6f} s, u = {u:.6f} m")
            break

        t += dt

    return t_list, u_list

# --- Simulation parameters ---
t_max = 0.5
dt = 1.0e-4

# Run both simulations
t_plastic, u_plastic = Euler_with_plastic(t_max, dt)
t_elastic, u_elastic = Euler_without_plastic(t_max, dt)

# Plotting comparison
plt.figure(figsize=(10,6))
plt.plot(t_plastic, u_plastic, label='With Plasticity (u_pl)')
plt.plot(t_elastic, u_elastic, label='Without Plasticity (No u_pl)', linestyle='--', color =
    'green')
plt.axhline(u_pl, color='orange', linestyle='--', label='Plastic region start (u_pl)')
plt.axhline(-u_pl, color='orange', linestyle='--')
plt.axhline(u_fail, color='red', linestyle='--', label='Failure displacement (u_fail)')
plt.axhline(-u_fail, color='red', linestyle='--')
plt.xlabel('Time (s)')
plt.ylabel('Displacement (m)')
plt.title('Wall Response Comparison: With vs Without Plasticity')
plt.grid()
plt.legend(loc='center left', bbox_to_anchor=(1, 0.5))
```

```
117 plt.tight_layout()
118 plt.subplots_adjust(right=0.75)
119 plt.savefig("Showcasing␣plasticity.png")
120 plt.show()
```

E

Displacement-time Curves for Various Explosives

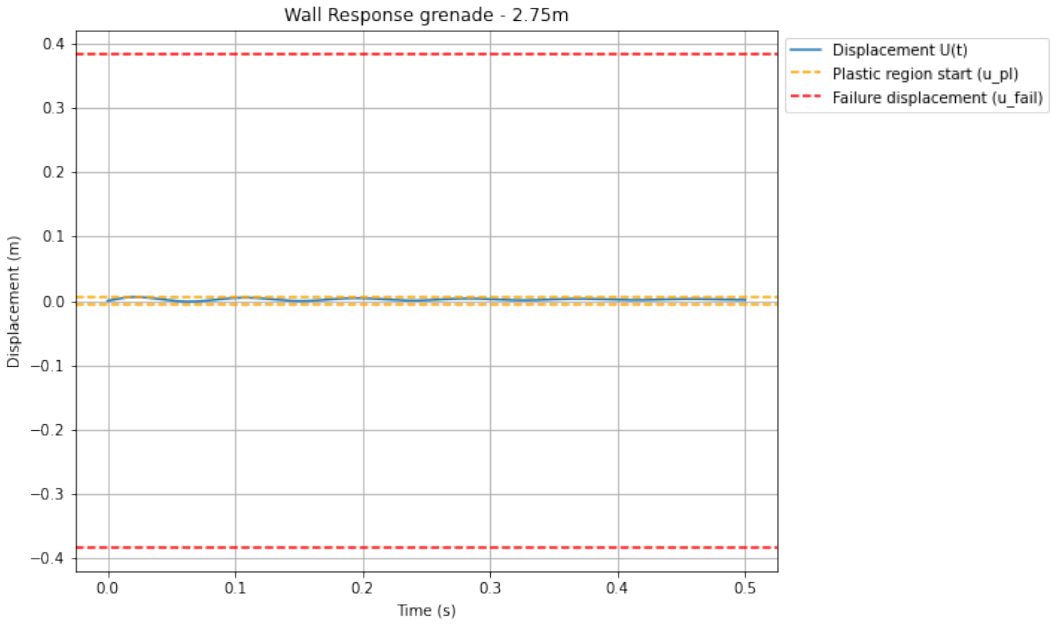

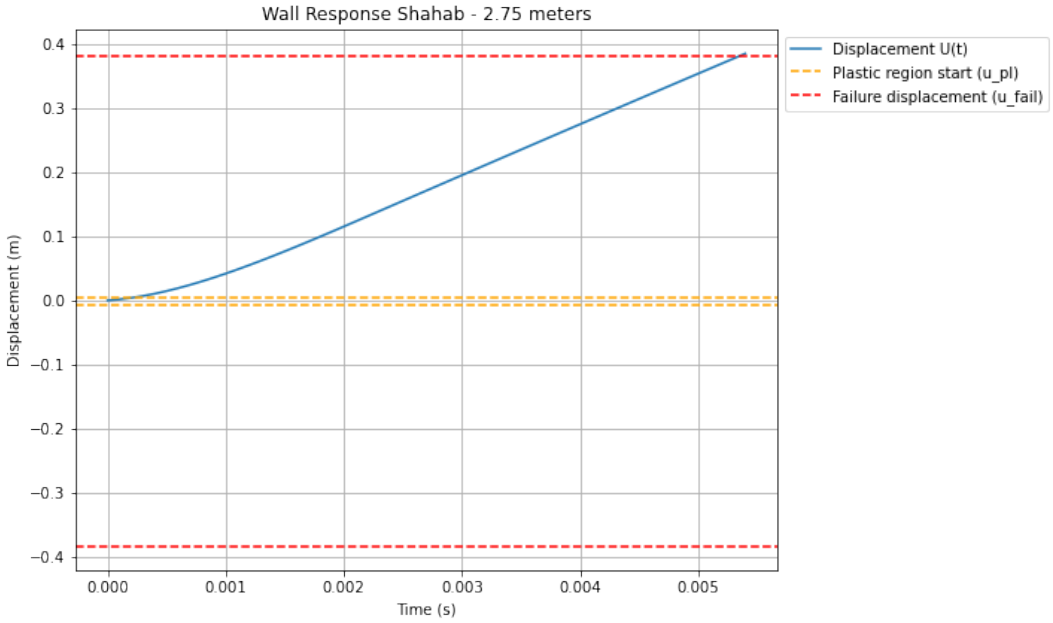
Wall Response Shahab - 2.75 meters
Displacement U(t)
Plastic region start (u_pl)
Failure displacement (u_fail)
Displacement (m)
Time (s)
0.4
0.3
0.2
0.1
0.0
−0.1
−0.2
−0.3
−0.4
0.000
0.001
0.002
0.003
0.004
0.005

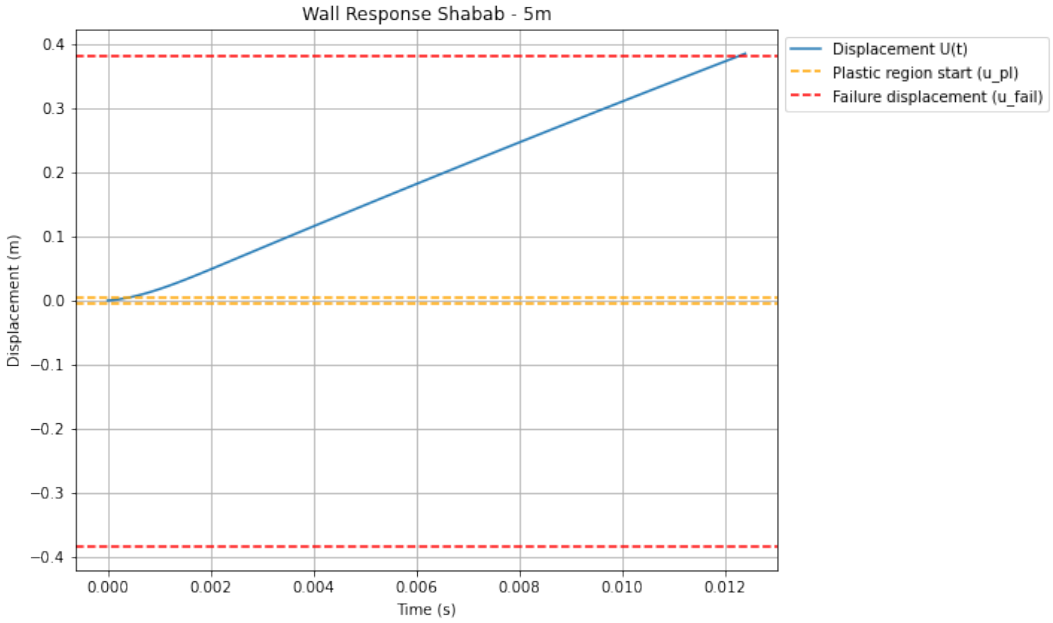
Wall Response Shabab - 5m
Displacement U(t)
Plastic region start (u_pl)
Failure displacement (u_fail)
Displacement (m)
Time (s)
0.4
0.3
0.2
0.1
0.0
−0.1
−0.2
−0.3
−0.4
0.000
0.002
0.004
0.006
0.008
0.010
0.012

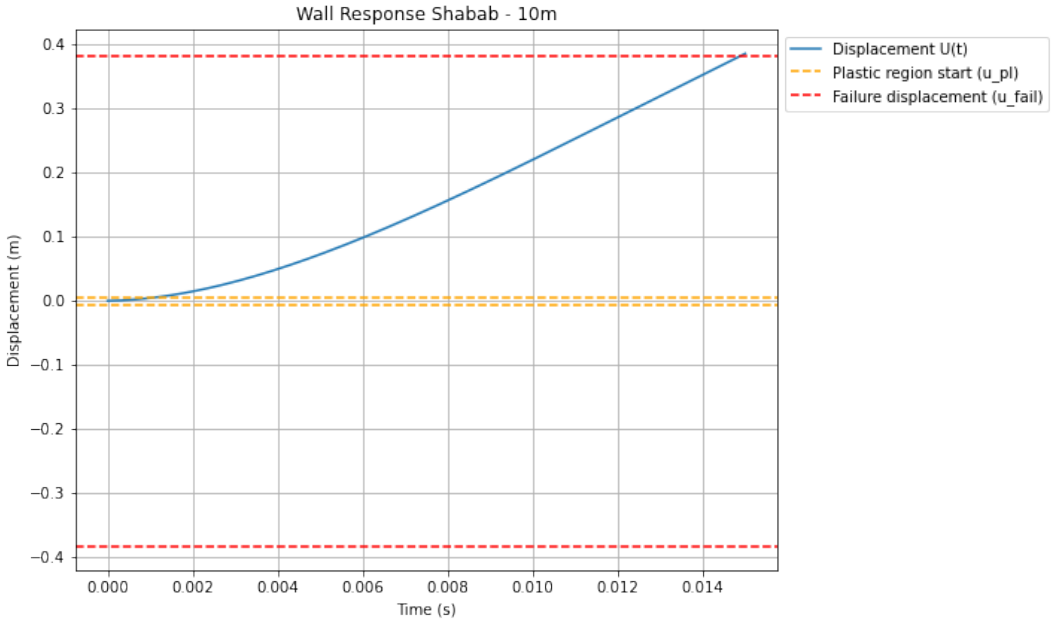
Wall Response Shabab - 10m
Displacement U(t)
Plastic region start (u_pl)
Failure displacement (u_fail)
Displacement (m)
Time (s)
0.4
0.3
0.2
0.1
0.0
−0.1
−0.2
−0.3
−0.4
0.000
0.002
0.004
0.006
0.008
0.010
0.012
0.014

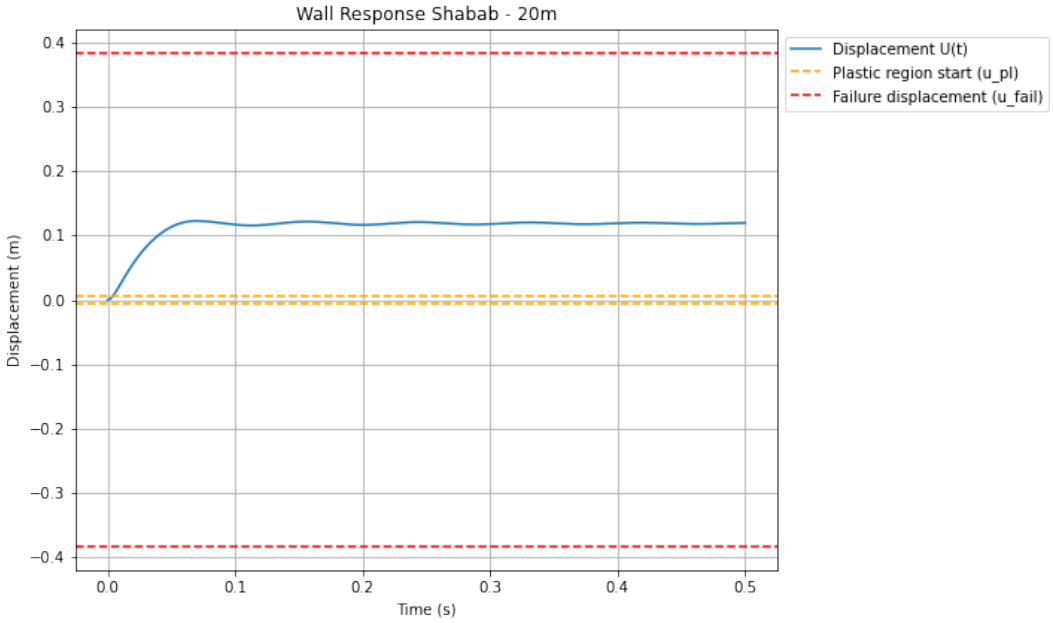
Wall Response Shabab - 20m
Displacement U(t)
Plastic region start (u_pl)
Failure displacement (u_fail)
Displacement (m)
Time (s)
0.4
0.3
0.2
0.1
0.0
−0.1
−0.2
−0.3
−0.4
0.0
0.1
0.2
0.3
0.4
0.5

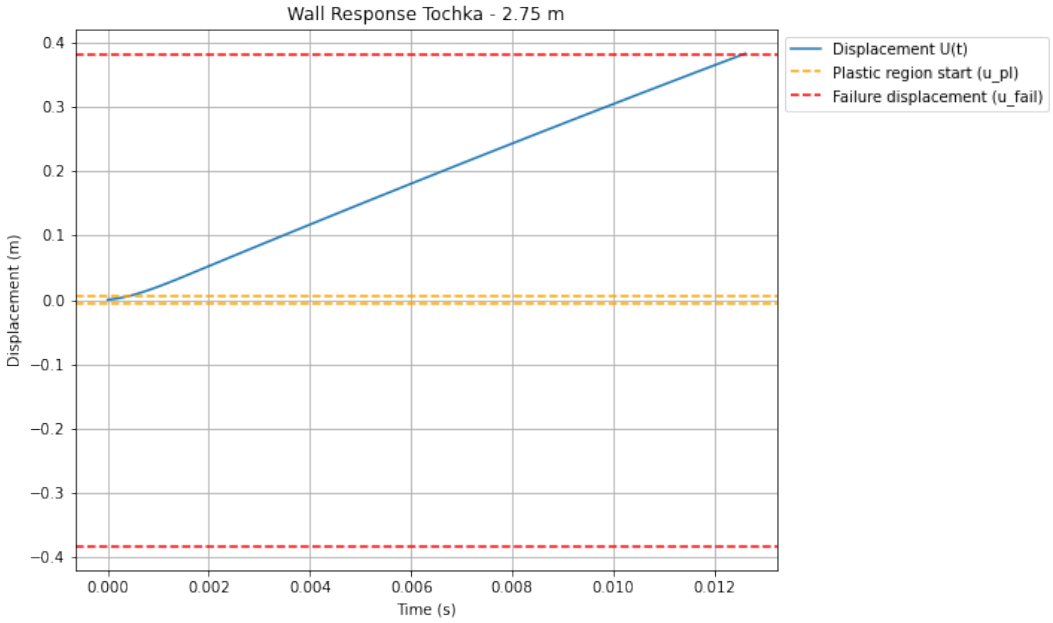
Wall Response Tochka - 2.75 m
Displacement U(t)
Plastic region start (u_pl)
Failure displacement (u_fail)
Displacement (m)
Time (s)
0.4
0.3
0.2
0.1
0.0
−0.1
−0.2
−0.3
−0.4
0.000
0.002
0.004
0.006
0.008
0.010
0.012

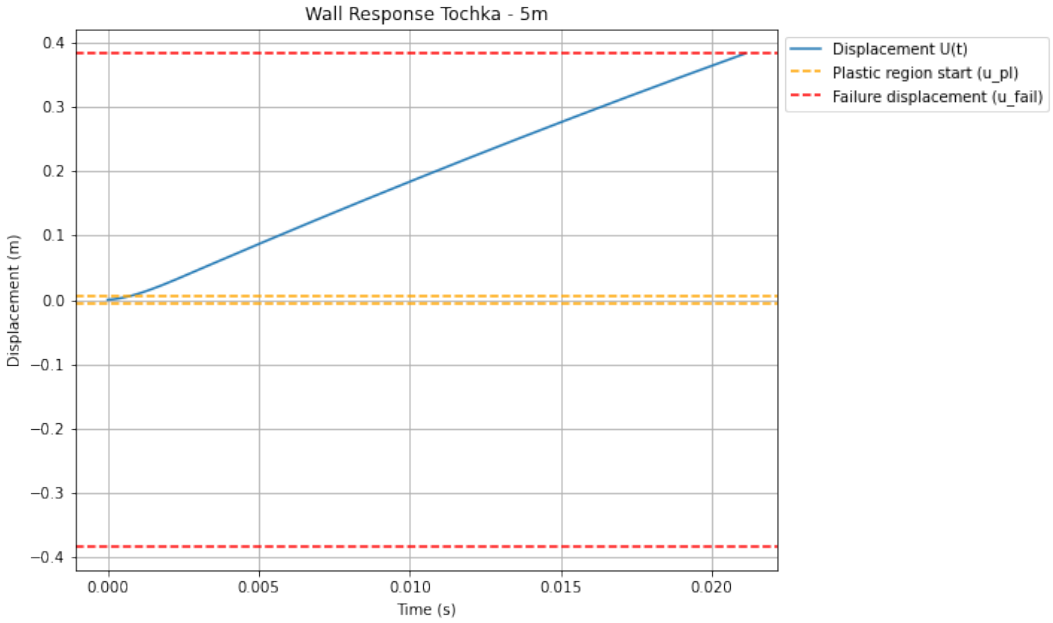
Wall Response Tochka - 5m
Displacement U(t)
Plastic region start (u_pl)
Failure displacement (u_fail)
Displacement (m)
Time (s)
0.4
0.3
0.2
0.1
0.0
−0.1
−0.2
−0.3
−0.4
0.000
0.005
0.010
0.015
0.020

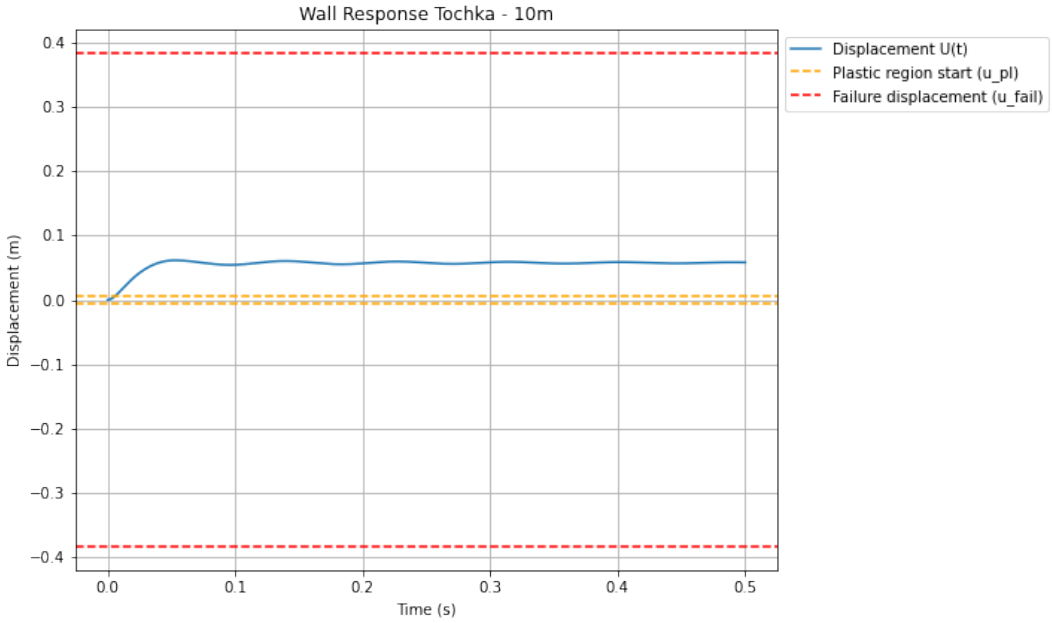
Wall Response Tochka - 10m
Displacement U(t)
Plastic region start (u_pl)
Failure displacement (u_fail)
Displacement (m)
Time (s)
0.4
0.3
0.2
0.1
0.0
−0.1
−0.2
−0.3
−0.4
0.0
0.1
0.2
0.3
0.4
0.5